



## Detailed tectonic evolution of the Reykjanes Ridge during the past 15 Ma

Á. Benediktsdóttir

*Department of Geology and Geophysics, University of Hawai'i at Mānoa, 1680 East-West Road, Honolulu, Hawaii 96822, USA (asdis@hawaii.edu)*

*Hawai'i Institute of Geophysics and Planetology, University of Hawai'i at Mānoa, Honolulu, Hawaii 96822, USA*

*Nordic Volcanological Center, Institute of Earth Sciences, University of Iceland, 101 Reykjavik, Iceland*

R. Hey and F. Martinez

*Hawai'i Institute of Geophysics and Planetology, University of Hawai'i at Mānoa, Honolulu, Hawaii 96822, USA*

Á. Höskuldsson

*Institute of Earth Sciences, University of Iceland, 101 Reykjavik, Iceland*

[1] We present a new detailed tectonic model of the Reykjanes Ridge which examines the rift propagation hypothesis for the V-shaped ridges and its asymmetric lithospheric accretion. Four major southward rift propagations extend through our entire survey area and several additional small scale rift propagations are observed, including northward propagators. If plume pulses only drive southward propagators, then two different driving mechanisms for propagators must exist. There is a major difference in the crustal accretion asymmetry between the area immediately off the Iceland shelf and that farther south, both in rift propagation pattern and free air gravity lineations. Furthermore, we identify two small offset features coined post-transforms, from which rift propagation is both initiated and stopped. The pattern of the V-shaped ridges on the Reykjanes Ridge is not symmetric about the Reykjanes Ridge and the V-shaped ridges are not linear continuous features. Our rift propagation model produces excellent fits to magnetic data and provides a self-consistent model for the evolution of the Reykjanes Ridge during the past 15 Ma.

**Components:** 7700 words, 13 figures, 8 tables.

**Keywords:** Reykjanes Ridge; plate tectonics; rift propagation.

**Index Terms:** 3035 Marine Geology and Geophysics: Midocean ridge processes; 3040 Marine Geology and Geophysics: Plate tectonics (8150, 8155, 8157, 8158).

**Received** 8 November 2011; **Revised** 9 January 2012; **Accepted** 9 January 2012; **Published** 18 February 2012.

Benediktsdóttir, Á., R. Hey, F. Martinez, and Á. Höskuldsson (2012), Detailed tectonic evolution of the Reykjanes Ridge during the past 15 Ma, *Geochem. Geophys. Geosyst.*, 13, Q02008, doi:10.1029/2011GC003948.

## 1. Introduction

[2] The Reykjanes Ridge (RR) is part of the Mid-Atlantic Ridge located in the North Atlantic between Iceland and the Bight Transform Fault near 57°N (Figure 1). It is a slow spreading ridge with a full spreading rate of  $\sim 20$  km/Myr along an azimuth of  $\sim 100^\circ$  [Merkouriev and DeMets, 2008; DeMets et al., 2010]. It is anomalous in many ways, including its oblique spreading of  $30^\circ$  from perpendicular to the ridge, and exhibiting a topographic axial high [Talwani et al., 1971] instead of the usual axial valley found at most slow spreading ridges. The axial high morphology has been attributed to excess melting due to a hot spot or a mantle plume beneath Iceland [Wilson, 1963; Morgan, 1971].

[3] The Reykjanes Ridge is also anomalous because of the diachronous topography and gravity V-shaped ridges (VSRs) flanking it (Figure 1). Vogt [1971] discovered this phenomenon and hypothesized that a plume underlying Iceland was pulsing, causing zones of thicker crust than normal during pulses, forming the ridges, and thinner crust in between pulses, forming the troughs. His hypothesis has since been taken as a fact and many models have been proposed to explain the pulses as asthenosphere or temperature pulses [e.g., Vogt and Johnson, 1972; White et al., 1995; White, 1997; White and Lovell, 1997; Smallwood and White, 1998, 2002; Albers and Christensen, 2001; Ito, 2001; Jones et al., 2002; Jones, 2003; Poore et al., 2006, 2009].

[4] One other model had previously been suggested for the origin of the V-shaped ridges. Hardarson et al. [1997] suggested that ridge relocations on Iceland [Sæmundsson, 1974] disrupt the flow of hot plume material to the RR [Hardarson et al., 1997, 2008], forming the troughs. In this model the Iceland plume is a steady state plume and it is the delivery of plume mantle material to the RR that changes in response to rift relocation on Iceland.

[5] Vogt [1971] concluded his discovery paper with the words ‘While the interpretation of V-shaped ridges as indicators of mantle flow seems promising, we do not claim that it is fact. Other propagating effects such as fractures and fluid instabilities should be explored’. Also, Johansen et al. [1984] and later Jones et al. [2002] observed an asymmetry in the VSRs about the RR and suggested that a more complicated explanation was necessary. Based on a 2007 survey of the RR and its flanks, Hey et al. [2010] proposed a model which is compatible with but does not require a mantle plume in which the VSRs are caused by a series of

propagating rifts migrating away from Iceland and producing asymmetry by transferring lithosphere from one plate to the other. Here we extend the initial results of Hey et al. [2010] and present a more detailed study of the propagating rift model of the Reykjanes Ridge.

## 2. Data

[6] In order to examine in greater detail the propagating rift model for the Reykjanes ridge we carry out detailed modeling of the magnetic data collected on R/V Knorr in June–July 2007. The ship tracks run nearly parallel to the spreading flowlines of the ridge predicted by the Eurasia–North America rotation parameters of C. DeMets (personal communication, 2010) (Figure 2). The magnetic profiles cover both the shallow Iceland shelf and deeper seafloor beyond it. The flatness of the Iceland shelf and its topographic step have been attributed to crustal flow caused by differences in zero-age crustal thickness [Jones and MacLennan, 2005]. Also, the magnetic anomalies become smooth and low in amplitude on the Reykjanes Ridge where it intersects the Iceland shelf [Talwani et al., 1971; Vogt et al., 1980]. Because of the structural complexities on the Iceland shelf we only model the off-shelf profiles 17–25 (Figure 1, survey box).

## 3. Methods

[7] We use a newly developed forward marine magnetic modeling program, Magellan (A. Benediktsdóttir et al., manuscript in preparation, 2012), to model our magnetic data. Magellan was developed in part to deal with some of the complexities of the Reykjanes ridge not treated in existing two-dimensional forward modeling programs, such as oblique spreading and an ability to handle an arbitrary number of ridge jump events. Below we discuss the various steps in the modeling process and then list the order in which they are executed.

### 3.1. Modeling Oblique Spreading Centers

[8] Two dimensional modeling of magnetic anomalies over an obliquely spreading ridge requires special treatment. First, data have to be collected along flowlines to actually match conjugate features (i.e., pseudofaults). By doing that the apparent width of the two dimensional magnetic blocks is larger than their actual width, as seen perpendicular to the strike of the ridge. In order to do the modeling in 2-D the flowline profiles must be projected orthogonal to

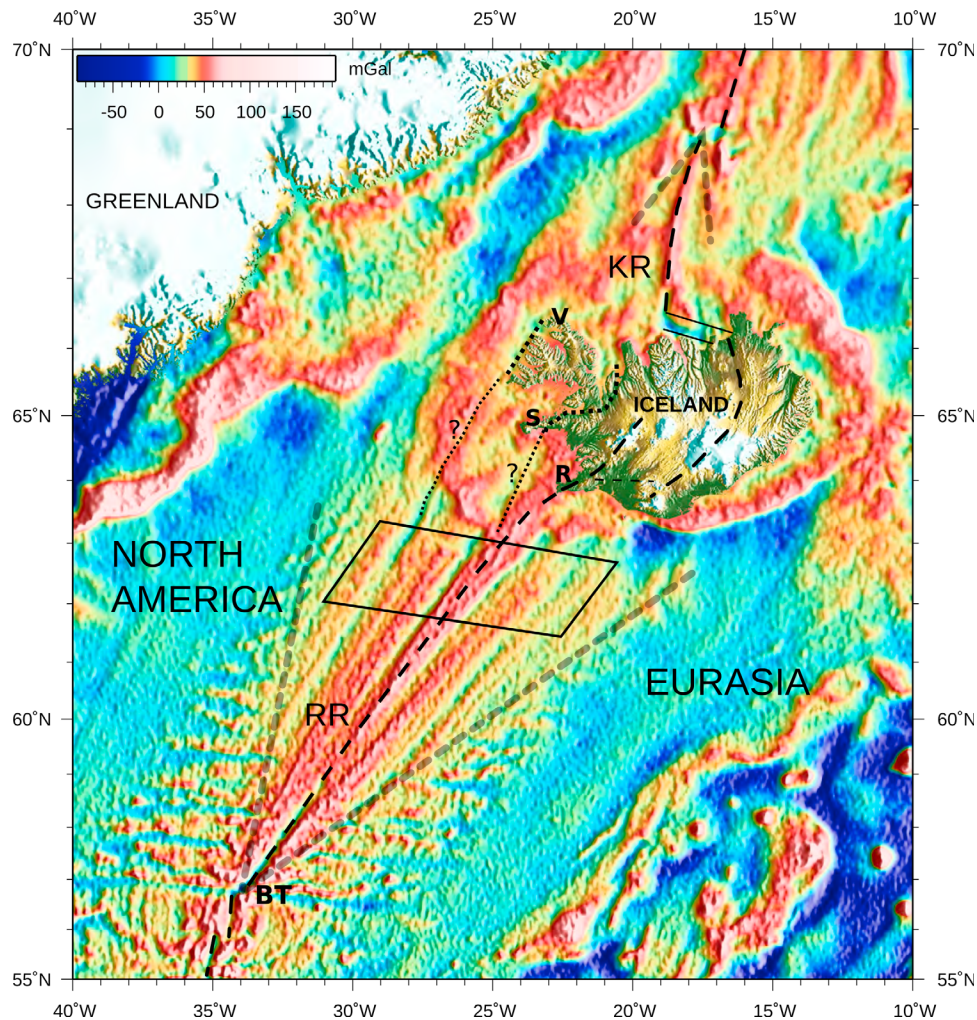


**Figure 1.** Satellite gravity and tectonic boundaries near Iceland [Sandwell and Smith, 2009] with gridded land topography superimposed. Heavy black dashes show Reykjanes Ridge (RR), Kolbeinsey Ridge (KR), and their extensions through Iceland. The VSRs we reinterpret here are the ridges and troughs slightly oblique to the Reykjanes Ridge axis enclosed by the southward pointing gray dashed V. Box shows location of profiles 17–25. Heavy dotted lines are paleo-spreading centers on Iceland and less heavy dotted lines show possible extensions down to our survey area. TFZ, Tjörnes Fracture Zone; V, Vestfirðir; S, Snæfellsnes; R, Reykjanes Peninsula; BT, Bight Transform. Modified from Hey *et al.* [2010].

the ridge to properly model the 2-D geometry of the magnetic body.

### 3.2. Contamination Coefficient

[9] At slow spreading ridges, such as the Reykjanes Ridge, the neovolcanic zone is broader compared to the ones at fast spreading ridges [Macdonald, 1977] and polarity transition zones are therefore more complex at slow spreading ridges, making the magnetic anomalies harder to identify (the magnetic blocks are not as wide and the broad transition zones affect the magnetic signal). This effect is not

accounted for in 2 dimensional models. The method of Tisseau and Patriat [1981], which describes the usage of the contamination coefficient, deals with this by simply narrowing the horizontal scale of the block model, thus changing the aspect ratio of the blocks and suppressing higher frequencies in the computed magnetic anomalies. This is a computationally simple and efficient procedure that mimics more complex geologic mechanisms, such as having a gradient in the magnetization polarity reversal which would simulate a zone of narrow alternating magnetization crustal emplacements which progressively change from one to the other polarity.

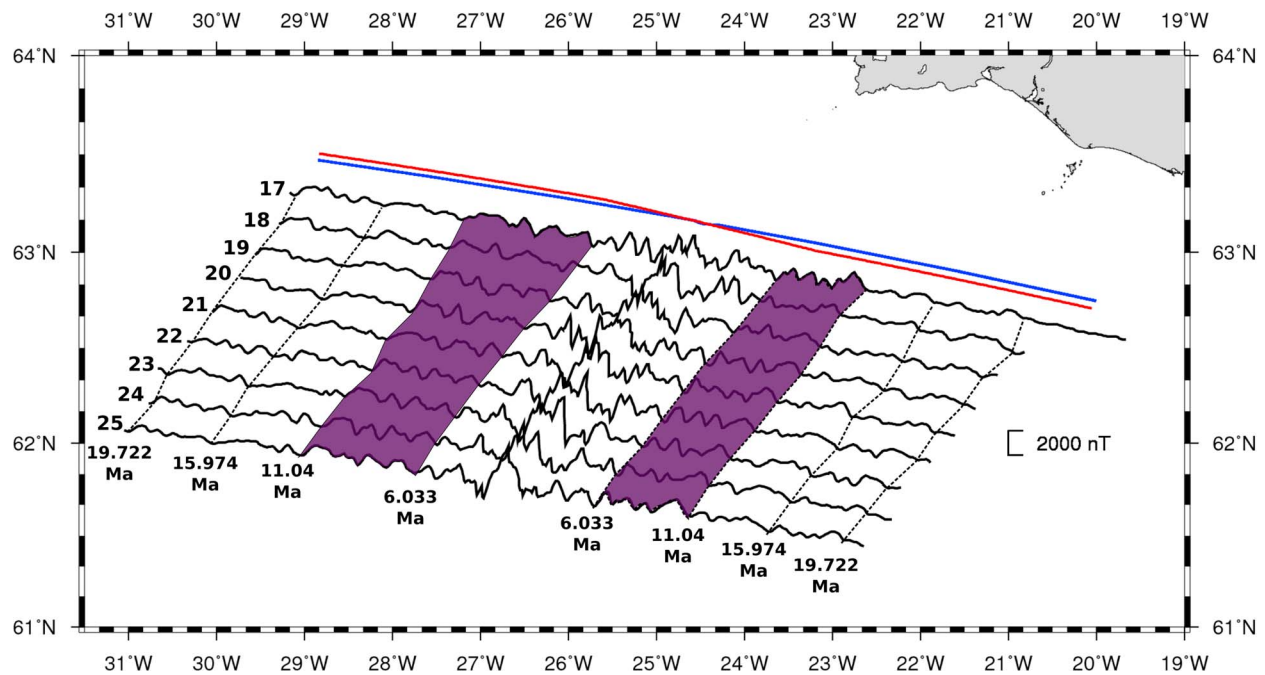


**Figure 2.** Magnetic data from the survey box in Figure 1. Dashed lines are magnetic anomalies used to define the new spreading rates for our magnetic modeling. Note the asymmetry of the anomalies, specifically there is more lithosphere between 6.033 Ma (chron 3r0 in work of *Lourens et al.* [2004]) and 11.04 Ma (chron 5n.2no in work of *Lourens et al.* [2004]) on North America than on Eurasia (shaded regions) and that asymmetry is independent of the ridge axis picks. Our ship tracks for profile 16 (blue line) and flowlines of the ridge predicted by the Eurasia–North America rotation parameters of DeMets (personal communication, 2010) (red lines) are shown. Our ship tracks are nearly parallel to the predicted flowlines and the difference between these two is negligible for magnetic modeling purposes. Profile numbers indicate the location of our profiles (17–25).

### 3.3. Outward Displacement

[10] Outward displacement comprises the effects which cause the youngest magnetic polarity zone to be wider than it would be if calculated from the actual spreading rate, and other polarity periods to be shifted away from the spreading center while maintaining their original width [*Atwater and Mudie, 1973; Hey et al., 1980; DeMets and Wilson, 2008*]. Intrusions of dikes into older crust of opposite polarity, older lava flows flowing over lava of opposite polarity and accumulation of gabbros under crust of opposite polarity are all processes that would cause the central Brunhes anomaly to be wider than true spreading rates predict. Outward displacement is therefore a source of error in global plate motion models and needs to be corrected for. It has been reported to be as high as 5–6 km on the Reykjanes Ridge [*DeMets and Wilson, 2008*].

[11] For the purposes of magnetic modeling the outward displacement is observed primarily in the central anomaly, causing the first spreading rate period to appear faster (wider) than it actually is. Later spreading stages would not be affected

because the outward displacement effect is canceled out (a reversal period is larger because of outward displacement while it is on the axis but as a new period starts it is shrunk because of the outward displacement of the new period) and all reversal boundaries would be displaced outward (hence the naming, *outward displacement*) so the older spreading rates would not change. The geometry of the outward displacement is not incorporated in our models as we use vertical polarity transition zones. This assumption is a likely source of misfit in our Brunhes anomaly modeling. The Brunhes anomaly is generally wider closer to Iceland which could be explained by increased outward displacement. Table 1 shows by how many kilometers the central anomaly is wider than the model central anomaly, when summed up for both flanks.

### 3.4. Modeling Procedure

1. The magnetic data should be collected along flowline profiles to ensure that the sampled features are indeed conjugate. This is particularly important where propagating ridges may be involved since

**Table 1.** Location of Ridge Axis and Total Difference Between the Model and Data Central Anomaly (Summed up From Both Ridge Flanks) for Profiles 17-25<sup>a</sup>

Profile	Latitude	Longitude	Central Anomaly Difference (km)
17	63.0027	-24.6786	8.5
18	62.8525	-24.9281	4.5
19	62.7050	-25.2071	7.0
20	62.5541	-25.4682	7.0
21	62.4071	-25.7432	5.0
22	62.2522	-25.9888	7.5
23	62.1037	-26.2715	5.0
24	61.9513	-26.5000	2.5
25	61.8012	-26.7803	2.0

<sup>a</sup>The data central anomaly is always wider and the uncertainty is always 1 km.

only flowline profiles will correctly match the geometry and timing of the conjugate pseudofaults.

2. The synthetic magnetized bodies (normal and reversed polarized blocks) are arranged according to spreading, jump, and asymmetry parameters. This is done in flowline space to ensure that the modeled anomalies are conjugate, i.e., that they formed at the same point on the axis.

3. The magnetized bodies are projected into a ridge-perpendicular space so that the two-dimensional assumption holds. The ridge is assumed to extend infinitely along its strike and it is therefore possible to use a 2-D method to calculate a magnetic model which arises from the magnetized ridge. Calculating the model from the magnetic blocks obtained from (2) would be equivalent to having the same ridge orientation but faster spreading (wider blocks). The width of the blocks in ridge-perpendicular space is what controls the width of the anomalies. The greater the obliquity the smoother the model will be because of the narrower width of the projected blocks measured in the ridge-perpendicular direction relative to the flowline direction. In general: the slower the spreading rate the smoother the model for purely geometrical reasons.

4. The contamination coefficient is applied to the synthetic magnetized bodies and to the distance scale on which the data are to be evaluated in perpendicular space.

5. The magnetic anomaly model is calculated in ridge-perpendicular space.

6. The magnetic anomaly model is projected back into flowline space where it is compared to the data. This involves only a horizontal stretching of the

calculated magnetic anomaly back to the original flowline geometry.

### 3.5. Picking the Axis Location

[12] In our magnetic data, propagating ridges are not detectable magnetically within the Brunhes chron. We therefore pick the axis in the middle of the observed central anomaly, that is the axis in the model is the time-averaged center of the Brunhes. If there is a recent propagating event the axis location should be systematically located on the Eurasia or North America side of the Brunhes. Our ridge axis picks for profiles 17–25 are given in Table 1.

## 4. Reykjanes Ridge Spreading Rates

[13] A fundamental part of forward magnetic modeling is the spreading rates used. They can be determined profile by profile, or predicted by the rotation parameters for the appropriate plate pair at the appropriate part of the ridge. The rotation parameters available are always found by inversions and they are thus best-fit values for a particular plate pair or global plate system. They do not take into account small scale complexities such as asymmetry caused by propagating rifts. Another critical issue is the spreading direction and its possible changes in time. The spreading direction defines the flowlines which are especially important in evaluating ridge propagation events. Unfortunately, the Reykjanes Ridge has no transform faults, which are the best source of information on spreading directions through time. Spreading directions are therefore largely constrained from more regional North Atlantic opening poles.

[14] A rotation pole for the North America - Eurasia plate pair from *Smallwood and White* [2002] (located at 66.85°N/135.46°E) was used to lay out our ship tracks which are compared to the flowlines predicted by a new rotation pole of DeMets (personal communication, 2010) (Table 2) in Figure 2. We assume our ship tracks are flowlines in this study as they are a good approximation of the newest predicted flowlines and to those of *Merkouriev and DeMets* [2008]. This will introduce an error to our pseudofault location equal to the distance between the ship tracks and the newest flowlines (0 at the axis and ~4 km past 6.733 Ma), assuming these latter ones are correct for this area.

[15] The techniques which are used to determine the rotation poles and angular rates [e.g., *Merkouriev and DeMets*, 2008; *DeMets et al.*, 2010] do not detect changes in spreading rate that are less than

**Table 2.** Stage Poles of Rotation for Eu-Na<sup>a</sup>

	0–6.733 Ma	6.733–11.04 Ma	11.04–15.974 Ma	15.974–19.722 Ma
	<i>DeMets (personal communication, 2010)</i>			
Latitude	63.76°N	68.81°N	68.81°N	68.81°N
Longitude	130.82°E	133.96°E	133.96°E	133.96°E
Rotation Angle	0.2133°/Myr	0.2734°/Myr	0.2734°/Myr	0.2734°/Myr
	<i>This Study</i>			
Latitude	66.85°N	66.85°N	66.85°N	66.85°N
Longitude	135.46°E	135.46°E	135.46°E	135.46°E
Rotation Angle	0.2251°/Myr	0.2600°/Myr	0.2762°/Myr	0.2550°/Myr

<sup>a</sup>Eurasia fixed.

1 km/Myr (DeMets, personal communication, 2010). In order to accurately model the magnetic data we need to refine the spreading rates on the Reykjanes Ridge.

[16] Figure 3 shows the crustal accretion for chrons 3ro (6.033 Ma), 5n2no (11.04 Ma), 5Bro (15.974 Ma),

and 6no (19.722 Ma) (all the chrons discussed here are from *Lourens et al.* [2004]), obtained from our magnetic data (black circles with error bars, from Table 3). By measuring the distance from the axis to these chrons on either side of the ridge and by summing the amount accreted on either side of the ridge the total amount of crust accreted along each

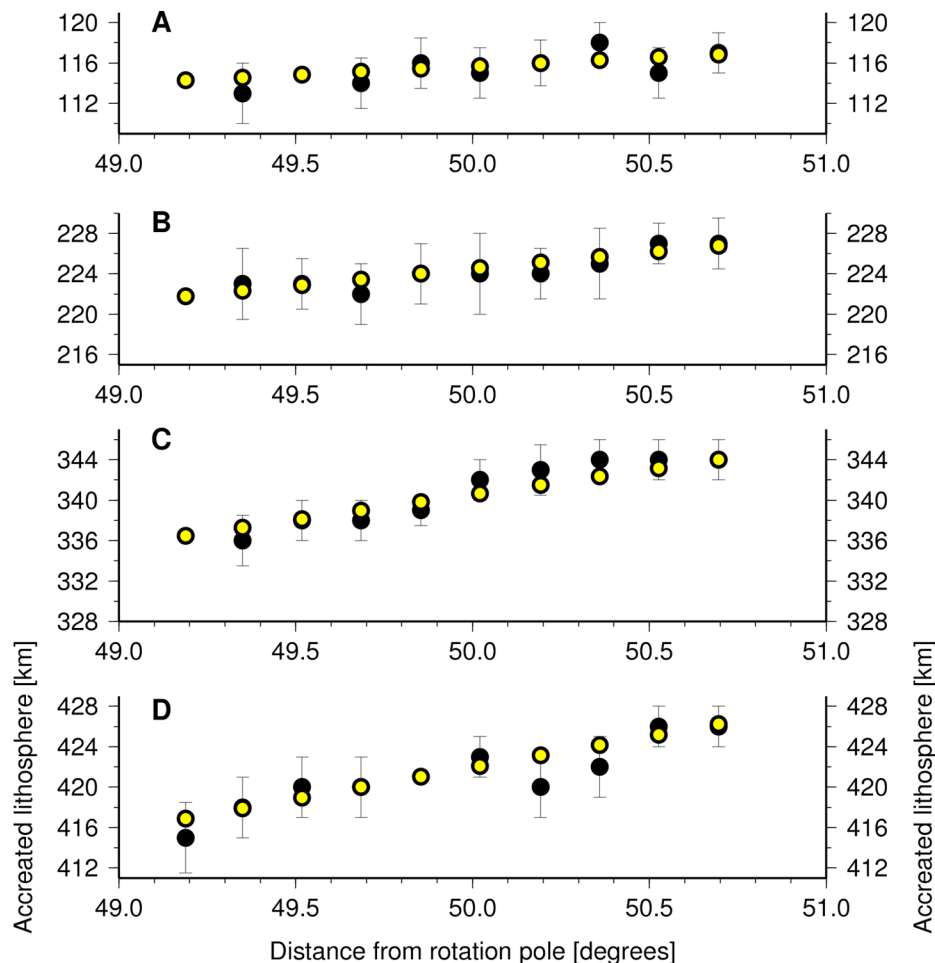


**Figure 3.** Total amount of accreted lithosphere (from Table 3) (black dots with error bars) and lithospheric accretion predicted by spreading rates from Table 4 (yellow dots) versus distance from rotation pole (from Table 2) at (a) 6.033 Ma, (b) 11.04 Ma, (c) 15.974 Ma, and (d) 19.722 Ma for tracks 17 (closest to pole) to 25 (farthest from pole).

**Table 3.** Distance of Anomalies From the Ridge in Kilometers

Profile	3ro (6.033 Ma)			5n.2no (11.04 Ma)			5Bro (15.974 Ma)			6no (19.722 Ma)		
	Na	Eu	Total	Na	Eu	Total	Na	Eu	Total	Na	Eu	Total
17	55 ± 2	58 ± 4	113 ± 7	122 ± 3	101 ± 4	223 ± 7	178 ± 3	158 ± 2	336 ± 5	222 ± 2	196 ± 4	418 ± 6
18	–	–	–	122 ± 3	101 ± 2	223 ± 5	177 ± 2	161 ± 2	338 ± 4	220 ± 3	200 ± 3	420 ± 6
19	54 ± 2	60 ± 3	114 ± 5	120 ± 2	102 ± 4	222 ± 6	177 ± 2	161 ± 2	338 ± 4	221 ± 2	199 ± 4	420 ± 6
20	57 ± 3	59 ± 2	116 ± 5	117 ± 3	107 ± 3	224 ± 6	176 ± 2	163 ± 1	339 ± 3	–	–	–
21	56 ± 3	59 ± 2	115 ± 5	116 ± 4	108 ± 4	224 ± 8	178 ± 3	164 ± 1	342 ± 4	221 ± 2	202 ± 2	423 ± 4
22	55.5 ± 2.5	60 ± 2	115.5 ± 4.5	115 ± 2	109 ± 3	224 ± 5	177 ± 3	166 ± 2	343 ± 5	220 ± 3	200 ± 3	420 ± 6
23	57 ± 2	61 ± 2	118 ± 4	117 ± 3	108 ± 4	225 ± 7	178 ± 2	166 ± 2	344 ± 4	220 ± 3	202 ± 3	422 ± 6
24	56 ± 3	59 ± 2	115 ± 5	118 ± 2	109 ± 2	227 ± 4	177 ± 2	167 ± 2	344 ± 4	220 ± 2	206 ± 2	426 ± 4
25	58 ± 2	59 ± 1	117 ± 4	118 ± 2	109 ± 3	227 ± 5	177 ± 2	167 ± 2	344 ± 4	221 ± 2	205 ± 2	426 ± 4

profile for each time was obtained, independent of the ridge axis pick. By using the location of the pole describing our ship tracks we find angular rates which predict a new set of improved spreading rates giving us predicted crustal accretion that best fits the data, minimizing the sum of squares (yellow circles in Figure 3). The new stage poles are given in Table 2. The new spreading rates, which we ultimately use in our magnetic models are given in Table 4 and shown in Figure 4.

[17] If we were to predict spreading rates profile by profile it would result in inconsistent spreading rates between profiles because of complexities such as variable outward displacement in the accretion process. Thus, the spreading rates would generally not increase exactly as the sine of the angular distance away from the location of the rotation pole, as demanded by rigid plate tectonics theory [Morgan, 1968]. Using spreading rates predicted by best-fitting poles of rotation for all of our profiles causes some imperfection in the forward magnetic modeling but it imposes spreading rate self-consistency between the profiles.

## 5. Reykjanes Ridge Accretion Asymmetry

[18] The asymmetric accretion of the Reykjanes Ridge is subtle as Vine [1966] did not mention it and

Talwani *et al.* [1971] and Herron and Talwani [1972] stated that the spreading was symmetric. Our initial modeling of the flowline magnetic profiles described above has found that the lithospheric accretion on the Reykjanes Ridge has not been symmetric for the past 20 Ma [Hey *et al.*, 2010]. Below we elaborate on different asymmetry-producing mechanisms and show that the propagating rift hypothesis is the most plausible one.

[19] Continuous asymmetric spreading, where more lithosphere is consistently added to one ridge flank over the other, has been proposed to occur in areas where asymmetrical accretion has been observed [Menard and Atwater, 1968; Weissel and Hayes, 1971; Hayes, 1976; Stein *et al.*, 1977]. Stein *et al.* [1977] suggested, by using a fluid mechanical model, that the trailing ridge flank with respect to the ridge migration direction would have a lower viscous dissipation rate and thus have a higher spreading rate. The ridge migration direction of the Reykjanes Ridge is to the northwest relative to Iceland [Hardarson *et al.*, 1997] and thus according to this model the Eurasia plate should accrete more material than the North America plate. Contrary to that prediction, the North American plate accreted more lithosphere between 6.733 and 19.722 Ma, although the Eurasian plate accreted a little more lithosphere between 0 and 6.733 Ma (see Table 3).

**Table 4.** Full Spreading Rates (km/Myr) Used in the Forward Magnetic Modeling

Profile	0–6.733 Ma	6.733–11.04 Ma	11.04–15.974 Ma	15.974–19.722 Ma
17	18.99	21.93	23.30	21.51
18	19.04	21.99	23.36	21.56
19	19.08	22.04	23.42	21.62
20	19.13	22.10	23.47	21.67
21	19.18	22.15	23.53	21.72
22	19.23	22.21	23.59	21.78
23	19.27	22.26	23.65	21.83
24	19.32	22.32	23.71	21.89
25	19.37	22.37	23.76	21.94

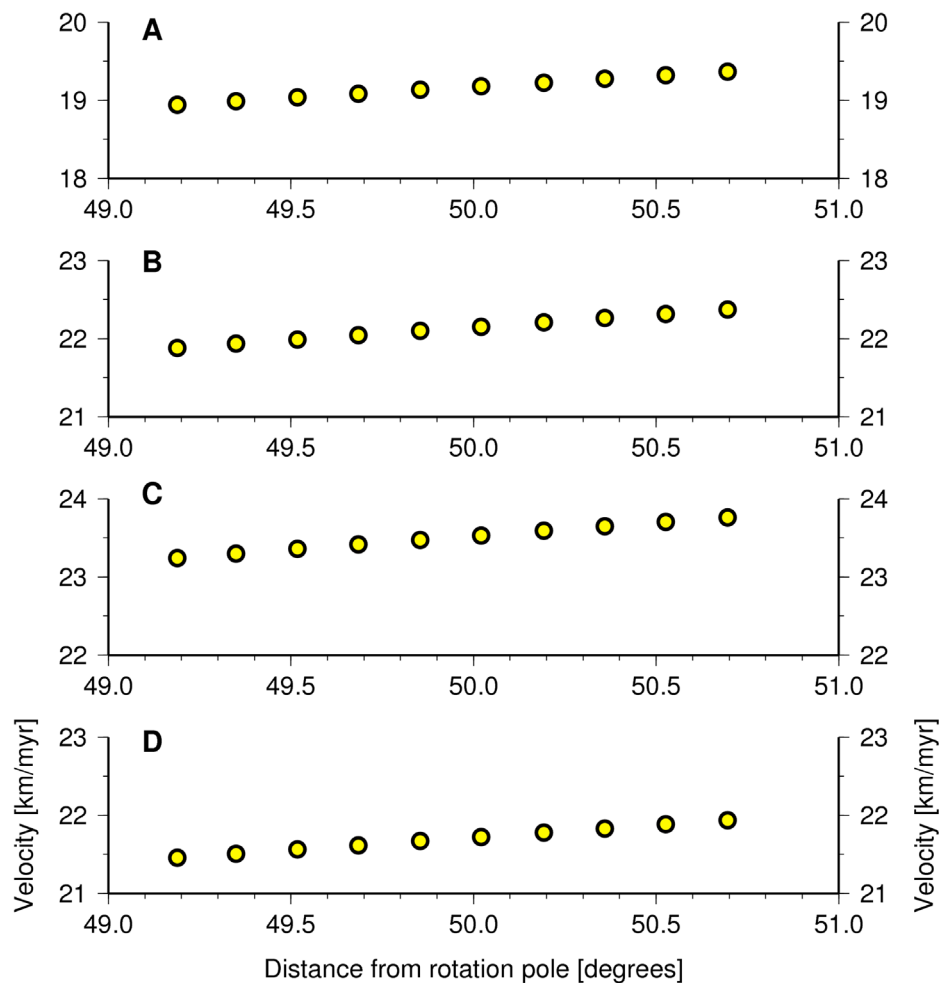


**Figure 4.** Spreading rates used in this study (from Table 4) versus angular distance from rotation pole (from Table 2) for (a) 0–6.733 Ma, (b) 6.733–11.04 Ma, (c) 11.04–15.974 Ma, and (d) 15.974–19.722 Ma for tracks 17 (closest to pole) to 25 (farthest from pole).

[20] If asymmetric accretion were uniform over many ridge segments asymmetry should be greater further away from the pole of rotation (the increase should follow the sine of the angular distance from the pole). In case of the Reykjanes Ridge, the asymmetry decreases away from the pole of rotation. Asymmetric accretion on the Reykjanes Ridge has not been uniform or in the same sense. It changes from accreting more lithosphere on the Eurasia plate during the past six million years to accreting more lithosphere on the North America plate 14 million years before that (see Table 3).

[21] Rift propagation has been shown to be the asymmetry producing mechanism in the classic areas where asymmetrical accretion has been observed. A ridge rotation model was proposed to be the source of asymmetry in the Northeast Pacific [Menard and Atwater, 1968] but the asymmetry producing

mechanism in their “Zed” area was later shown to be rift propagation [Caress *et al.*, 1988; Hey *et al.*, 1988]. Similarly, regional continuous asymmetric spreading was suggested to be the cause of the asymmetrical accretion in the Australia-Antarctic Discordance [Weissel and Hayes, 1971] which is now understood to be caused by rift propagation [Vogt *et al.*, 1983; Phipps Morgan and Sandwell, 1994; Christie *et al.*, 1998]. Furthermore asymmetrical accretion has been observed and attributed to rift propagation in the Juan de Fuca Area [Shih and Molnar, 1975; Wilson *et al.*, 1984], the Easter Microplate [Naar and Hey, 1991], Galapagos [Hey and Vogt, 1977; Hey *et al.*, 1980; Wilson and Hey, 1995] and on the Mid-Atlantic Ridge at ca. 26°–27°N [Kleinrock *et al.*, 1997]. A third asymmetric producing mechanism is by discrete ridge jumps but as there are very few well documented examples of this mechanism, and as the best studied area is in a

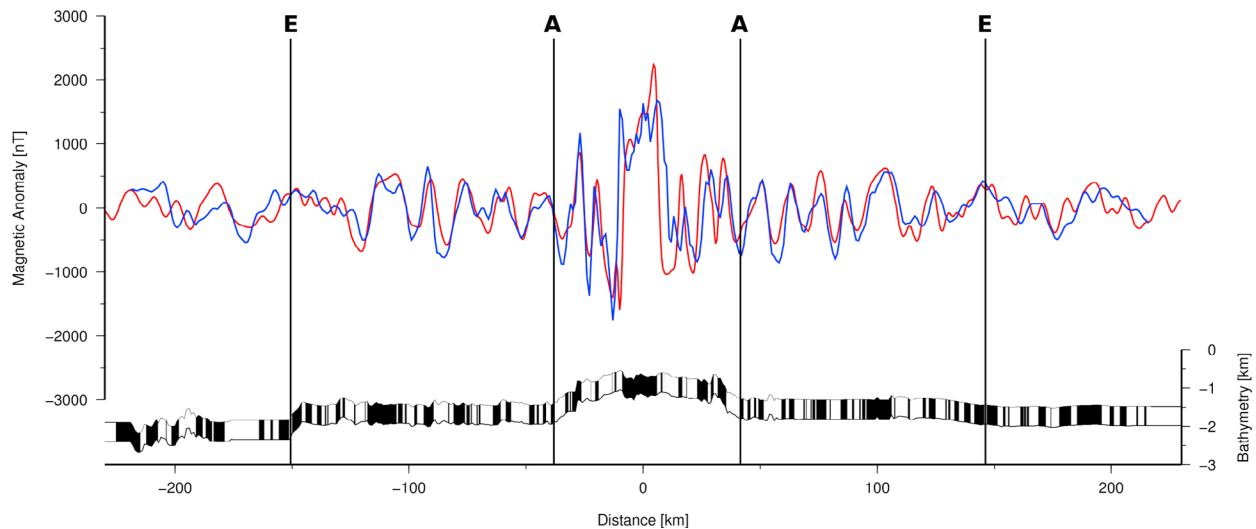


**Figure 5.** Profile 20 modeled with spreading rates shown in Table 4 and abrupt shifts in both magnitude and sense of asymmetry shown in Table 5. Blue is the data and red is the model. Black and white boxes are normal and reversed magnetized blocks, respectively, following the bathymetry. Note that the bathymetric A scarps and the E scarps are the same age on each side of the ridge (as indicated by the magnetic reversal sequence). Compare this fit with profile 20 modeled with ridge jumps in Figure 8d, where the fits are similar but mechanism more plausible.

back-arc basin (the Woodlark Basin) [Goodliffe *et al.*, 1997] we will not discuss this mechanism further.

[22] Figure 5 shows our profile 20 modeled using asymmetric spreading (the spreading rates and asymmetry are given in Tables 4 and 5, respectively). The fit of this model to the data is generally very good until 15.8 Ma when we use 53% asymmetry to the west (accreting more lithosphere to North America). This might partially be caused by the fact that we use best fitting spreading rates over all the profiles, instead of trying to fit spreading rates to individual profiles. However, the sense and amount of asymmetry are both required to change abruptly over a timescale of  $\sim 1$  Ma (see Table 5 and Figure 6). If this is indeed asymmetric spreading we can think of no plausible explanation for why the ridge would behave in such a way. Instead, we take it as a strong evidence for propagating rifts, which cause abrupt changes in asymmetric accretion by discrete ridge jumps. A good example where lithosphere is transferred first to one flank and then to the other by rift propagation is Galapagos [Wilson and Hey, 1995], where the 95.5W propagator is transferring lithosphere from the Nazca to the Cocos plate, while the 93W propagator following behind it is transferring lithosphere from the Cocos to the Nazca plate. Both are propagating west. A less-analogous example is Juan de Fuca, where southward propagators transferred lithosphere from the Pacific to the Juan de Fuca plate and northward propagators transferred lithosphere from the Juan de

Fuca to the Pacific plate [Hey and Wilson, 1982; Wilson *et al.*, 1984].

[23] For the reasons discussed above we prefer the well documented asymmetry producing mechanism, rift propagation, over continuous regional asymmetric accretion and discrete ridge jumps.

## 6. Propagating Rift Magnetic Modeling

### 6.1. How Propagating Rifts and Ridge Jumps Relate

[24] Figure 7 schematically shows a map view of a continuously propagating rift replacing a dying

**Table 5.** Percentage Asymmetry for Modeling of Profile 20 in Figure 5<sup>a</sup>

Time Period (Ma)	Asymmetry (%)
0–1	–20
1–2	0
2–3	5
3–3.8	45
3.8–4.8	–6
4.8–6.1	0
6.1–7	–20
7–8.2	–8
8.2–10.7	–18
10.7–13	16
13–14.9	0
14.9–17	–53
17–118	0

<sup>a</sup>Positive asymmetry indicates more accretion on Eurasia plate.

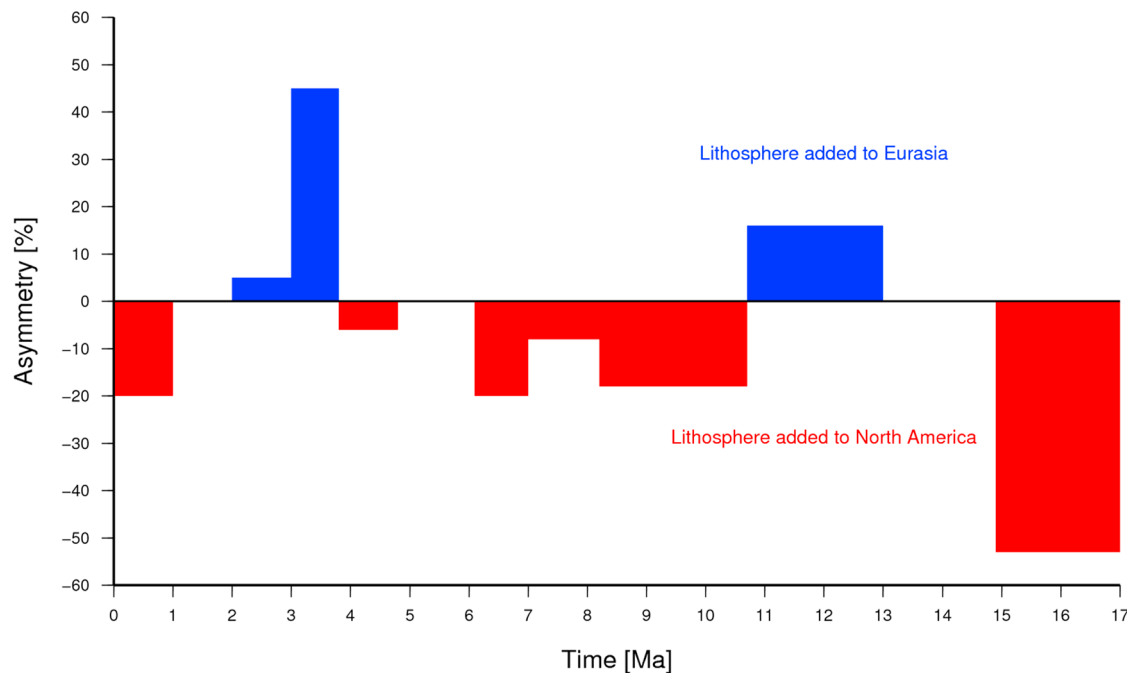


**Figure 6.** A schematic representation of the sense of asymmetric accretion for the model of profile 20 shown in Figure 5. The asymmetry values are given in Table 5. Positive and negative asymmetries represent more lithosphere added to the Eurasian plate and the North American plate, respectively.

ridge. As it does so lithosphere is transferred from plate B to plate A, causing the lithospheric accretion to be asymmetric. Two pseudofaults on each plate offset the magnetic lineations and the magnetic fabric is rotated in the zone of transferred lithosphere. Comparing magnetic data which are collected along the spreading flowlines of ridges where propagation has and has not occurred will not show the same pattern of magnetic anomalies. In the case where propagation has occurred the magnetic anomalies will look as if a chunk of one plate has been transferred over to the other, thus shuffling the magnetic anomalies around. This process can be imitated by incorporating a ridge jump parameter, to move lithosphere from one plate to the other, when forward calculating the magnetic field from synthetic magnetized blocks. The ridge jump is treated as an instantaneous event in the magnetic models. A propagating rift and ridge jumps are closely related phenomena, looked at from different view points - the ridge jumps observed on individual profiles are caused by new rifts propagating quasi-orthogonally to the profiles [Hey *et al.*, 1980].

## 6.2. Prior Results of Hey *et al.* [2010]

[25] The new propagating rift model of Hey *et al.* [2010] shows that an alternative mechanism exists

for the origin of the V-shaped ridges south of Iceland. Hey *et al.* [2010] found a self-consistent pattern of jumps that produces most of the observed asymmetric accretion and provides generally good fits to the magnetic anomalies. Each jump results from a propagating rift, traveling away from Iceland. The jump boundaries coincide with linear VSR boundaries, strongly suggesting the VSRs are propagating rift wakes. The data analysis by Hey *et al.* [2010], however, is imperfect as they always fit one ridge flank better than the other and they do not use the newest poles of rotation (DeMets, personal communication, 2010) to impose a self-consistent spreading rate pattern. Their jump pattern is therefore rather a rough outline of what we observe, rather than a detailed history.

## 6.3. Assumptions

[26] In our magnetic modeling we assume that the A-scarps are of the same age. The A-scarps are two tectonic-looking scarps, on either side of the ridge (Figure 5), facing away from the axis. Although they had been thought to be symmetric about the axis [Vogt, 1971], they are not the same distance away from the axis when measured along spreading flowlines [Hey *et al.*, 2010]. How could two large scarps with similar characteristics, on either side of the ridge, be created at different times? The question

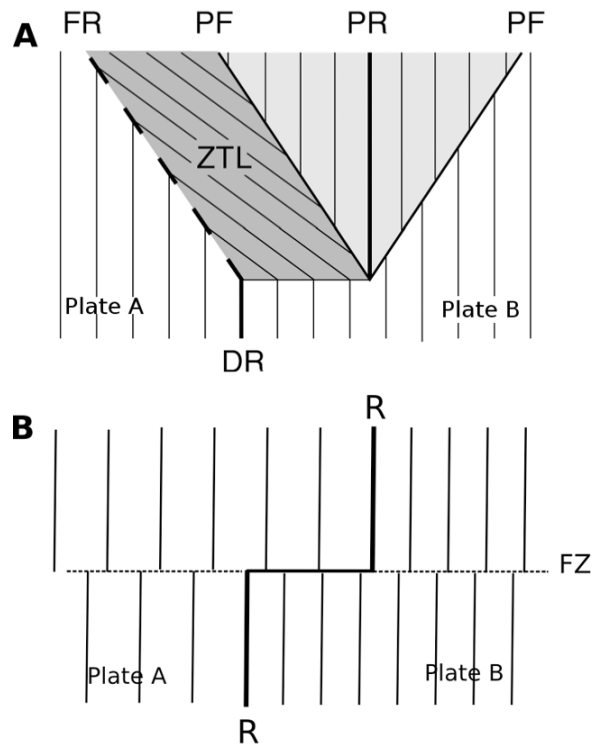


**Figure 7.** Schematic comparison between two asymmetry-producing mechanisms, (a) propagating rift and (b) asymmetric spreading. Figure 7a: map view of a propagating rift (PR) after *Hey et al.* [1980]. The PR propagates down and replaces the dying rift (DR), producing two pseudofaults (PF), a failed rift (FR) and zone of transferred lithosphere (ZTL) where lithosphere was moved from plate B to plate A, producing asymmetric accretion. Thin vertical lines are isochrons, rotated in the ZTL. A cross-sectional profile perpendicular to the strike of the ridge would show the failed rift outside the pseudofault on plate A. Figure 7b: two asymmetric spreading ridge segments (R) are offset by a transform fault. Asymmetric spreading produces no V-shaped pattern. Isochrons are farther apart on plate A than plate B because of asymmetric spreading. Thin vertical lines are isochrons, offset by a fracture zone (FZ).

is therefore not “why are they the same age”, but “how could scarps be the same age yet different distances from the axis?” Within the bounds of the A-scarp there is more lithosphere on the Eurasia side than on the North America side and the asymmetry increases toward Iceland, as seen by the jump parameters in Table 6.

[27] Our magnetic models have simple vertical polarity transition zones giving rise to imperfect fits to the central anomaly, specifically closer to Iceland where the central anomaly widens. Incorporating the geometry of outward displacement to our models

could improve the fits to the central anomaly; one would need to define new spreading rates based on a pole of rotation corrected for outward displacement (DeMets, personal communication, 2010).

#### 6.4. Magnetic Models

[28] Figure 8 shows the magnetic models for tracks 17–25 modeled with the spreading rates in Table 4 and the jump and magnetization parameters in Table 6. Our models use a contamination coefficient of 0.5–0.7, as seen in Table 6.

[29] The fit to the data is very good for profiles 19–25. These profiles are farther from the shelf than profiles 17 and 18 which are located in the transition zone between the shelf and the ridge. The fits to profiles 17 and 18 have however been significantly improved from the ones found by *Hey et al.* [2010] where specifically profile 18 was not fitted well.

[30] The size of the jumps is constrained to  $\approx 0.2$  km whereas the time of the jumps is constrained to  $\approx 0.5$  Ma (0.5 Ma with a half spreading rate of  $\approx 10$  km/Myr = 5 km). As mentioned before we take our ship tracks to be the flowlines of the ridge. Our ship tracks and the newest predicted flowlines are maximum 4 kilometers apart and this assumption should therefore not change our overall results, rather alter the pseudofault location pattern slightly. Note that one could split up a single jump to two jumps or more, if desired, but that increases the free parameters used in the modeling making it statistically less significant.

[31] When modeling magnetic anomalies we start at the ridge axis and then move out to the ridge flanks because the younger parameters affect the older magnetic anomaly pattern. In order to figure out what size of jumps to put in the modeling for a specific time range we need to view magnetic anomalies that are a few million years older to see how the younger jump affects the older portion of the magnetic data. For this reason we have only modeled our data out to  $\sim 15$  Ma even though the data range is out to  $\sim 20$  Ma, which explains some of the misfit to the data between  $\sim 15$  Ma and  $\sim 20$  Ma.

[32] Table 7 shows the root mean square error between the magnetic model and observed data, for this study and those of *Hey et al.* [2010]. In magnetic modeling most of the signal is a short wavelength and a small shift can produce a large residual, which explains the big difference in these two studies. The new models we present here reduce

**Table 6.** Parameters Used for the Forward Magnetic Modeling<sup>a</sup>

Profile	Jumps		Magnetization		
	Time of Jump (Ma)	Distance (km)	Interval (Ma)	Magnetization (A/m)	
17 c = 0.6	1.7	-4.0	0-0.78	20	
	2.35	-8.0	0.78-15	6	
	4.5	-4.1	15-20	4	
	6.4	13.0			
	7.7	6.0			
	8.8	3.0			
	10.5	1.5			
	12.2	-4.0			
	13.0	5.0			
	14.5	4.0			
	18	1.6	-4.0	0-0.78	20
	c = 0.5	2.6	-7.5	0.78-15	8
		4.1	-4.0	15-20	5
		5.8	15.0		
7.7		6.0			
8.5		2.5			
10.0		1.2			
11.5		-6.0			
13.2		3.0			
14.5		4.8			
19		2.1	1.1	0-0.78	20
c = 0.7	3.5	-4.5	0.78-15	6	
	6.0	4.0	15-20	6	
	8.3	4.7			
	10.0	2.0			
	11.8	-5.0			
	14.4	7.5			
	20	1.9	0.9	0-0.78	20
c = 0.5	3.2	-2.3	0.78-15	8	
	6.6	3.0	15-20	6	
	8.2	1.7			
	10.0	1.5			
	12.0	-3.8			
	14.4	5.0			
	21	1.9	1.4	0-0.78	25
c = 0.7	3.0	-2.2	0.78-15	8	
	6.7	3.0	15-20	6	
	8.0	2.5			
	12.3	-3.8			
	14.3	7.5			
	22	1.7	0.6	0-0.78	30
c = 0.7	2.4	-3.5	0.78-15	8	
	6.9	3.4	15-20	6	
	7.7	1.4			
	10.8	1.5			
	13.4	3.4			
	23	1.3	1.2	0-0.78	30
c = 0.7	2.4	-3.9	0.78-15	8	
	6.1	2.8	15-20	6	
	7.5	1.8			
	10.5	2.6			
	13.2	2.1			
	24	1.3	1.3	0-0.78	30
	c = 0.7	2.4	-3.9	0.78-15	8
6.4		2.5	15-20	6	
7.5		2.2			
10.5		1.6			
13.0		3.3			

**Table 6.** (continued)

Profile	Jumps		Magnetization	
	Time of Jump (Ma)	Distance (km)	Interval (Ma)	Magnetization (A/m)
25	0.9	0.8	0-0.3	40
c = 0.5	1.8	-2.6	0.3-0.78	25
	6.6	2.1	0.78-15	10
	7.2	2.3	15-20	6
	10.5	0.8		
	13.0	3.0		

<sup>a</sup>Abbreviation: c, contamination coefficient.

the RMS misfit compared to that of *Hey et al.* [2010] by the amounts shown in Table 7.

## 7. Results

[33] Figure 9 shows time of jump versus distance away from Iceland compiled for profiles 17–25. Propagation has occurred both away from and toward Iceland, as indicated by the arrows, where lithosphere is transferred to Eurasia (blue dots) or North America (red dots). The size of jumps is indicated by the area of the dots. The southward propagators tend to extend all the way through the survey area while the northward propagators tend to be shorter and less pronounced. This is plausibly associated with a topographic gradient away from Iceland [*Searle et al.*, 1998] which the southward propagators need not overcome like the northward propagators. Also, the pattern of propagators is likely complicated by the growth and evolution of the axial volcanic ridges which form sub-normal to the spreading direction and can propagate to off-axis lithosphere [*Searle and Laughton*, 1981; *Parson et al.*, 1993; *Searle et al.*, 1998].

[34] Figures 10 and 11 show snapshots of the evolution of the propagating rift history of the Reykjanes Ridge implied by the magnetic anomaly fits in Figure 8. Figure 10 shows a schematic evolution of the Reykjanes Ridge where our southernmost profile 25 is at  $y=290$  km and the Reykjanes Peninsula is at  $y=0$  km. The  $y$ -axis runs perpendicular to the flowlines of the ridge so the positive azimuth of the  $x$ -axis is  $100^\circ$  clockwise from north. Pseudofaults of southward and northward propagating rifts are connected with blue and green lines, respectively. Figure 11 shows the evolution in a map view on top of satellite gravity [*Sandwell and Smith*, 2009]. Pseudofaults of southward and northward propagating rifts are connected with solid and dashed lines, respectively. Table 8 shows the

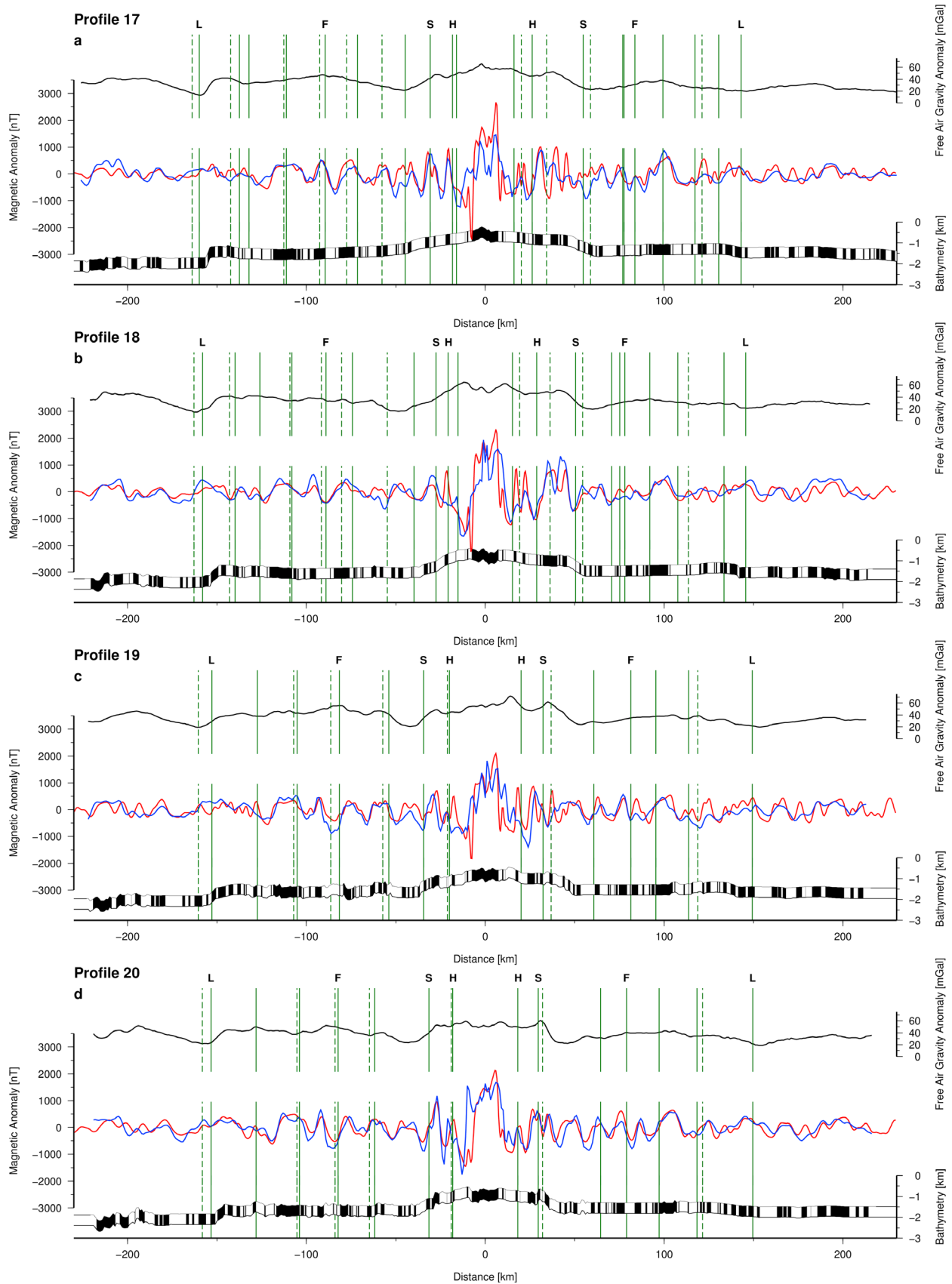


Figure 8

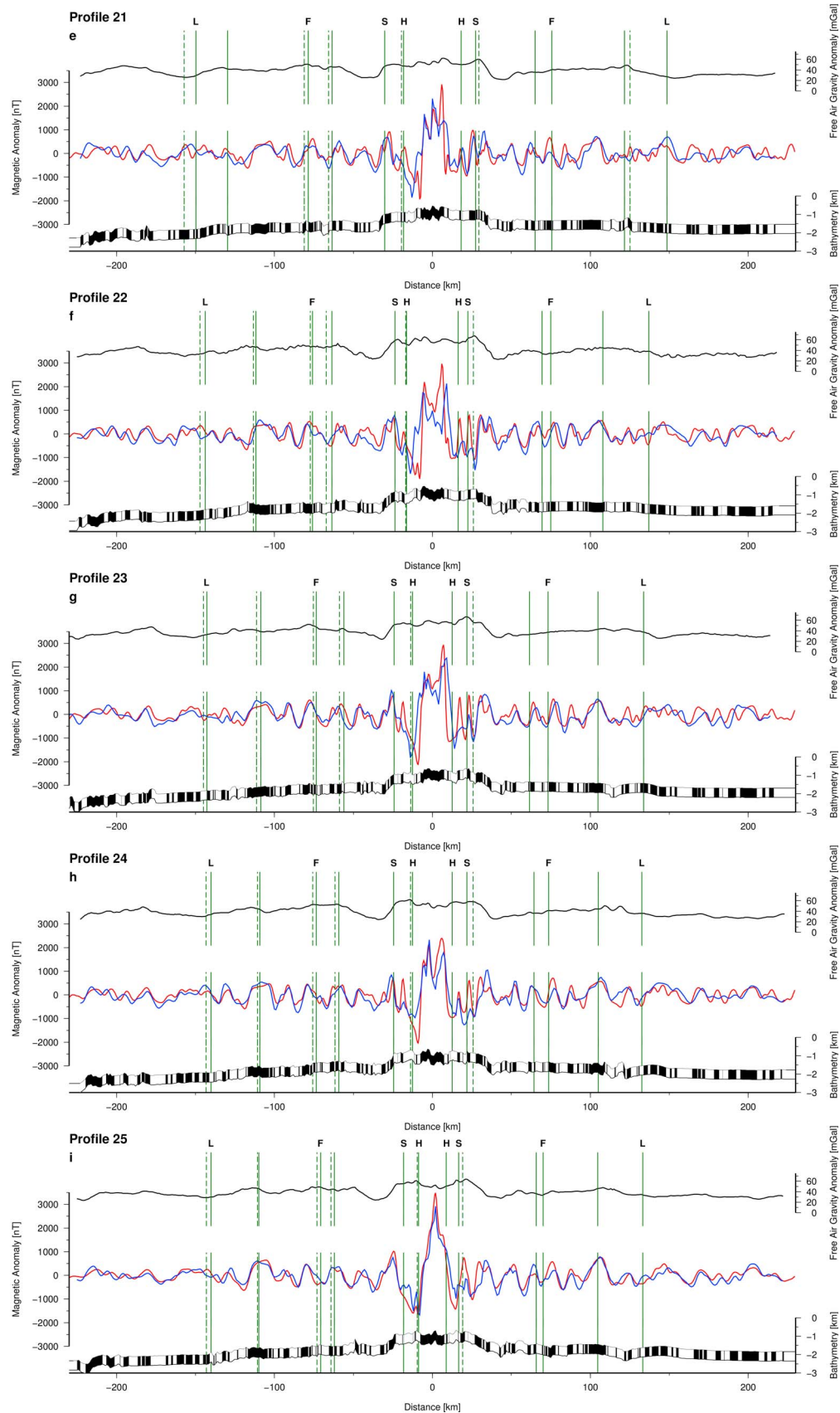


Figure 8. (continued)

**Table 7.** Magnetic Modeling RMS Misfit Values From This Study and *Hey et al.* [2010]

Profile	This Study (nT)	<i>Hey et al.</i> [2010] (nT)	Reduction in RMS (%)
17	348	368	5
18	346	478	28
19	370	423	13
20	332	431	23
21	352	391	11
22	430	475	9
23	393	439	10
24	295	390	24
25	262	379	31

different naming conventions between this study and that of *Hey et al.* [2010].

[35] We divide our survey area into two sub-areas; profiles 17 and 18 are located where the Reykjanes Ridge meets the Iceland shelf and the crustal accretion appears to be more complex than in the profiles to the south. Below we review the tectonic evolution of these two sub-regions as well as a detailed discussion of the methods used to produce the reconstruction snapshots.

### 7.1. Reconstruction Movies

[36] To reconstruct the plate spreading we cut the gravity grid between the span of profiles 17 and 25 and the time span between 19 Ma and the time of the snapshot, on both ridge flanks. We found the exact location of the desired age on the gravity grid by putting a fictitious zero-distance jump at the snapshot time into Magellan for each of the profiles. We ran Magellan with the modeling parameters from Table 6 and spreading rates from Table 4 giving us an exact location (longitude, latitude coordinates) of the time-marker (that way we are not assuming symmetric accretion).

[37] To rotate the gravity grid we use the stage poles we found earlier (Table 2). Note that these reconstructions are independent of the present-day ridge axis location. The ridge axis location at each snapshot is therefore generally not exactly the same as the ridge axis location in present-day.

[38] The reconstruction animations can be found at <http://www.youtube.com/watch?v=JcFgHxXKMdo>

and <http://www.youtube.com/watch?v=KDIhK68OqAw> (see Animations S1 and S2 in the auxiliary material).<sup>1</sup>

### 7.2. Profile 19 and South

[39] Clear history of propagating rifts is revealed for profiles 19–25 in Figure 9. Four southward propagating rifts extend through our entire survey area and can be traced back to Iceland. The oldest propagator left Iceland at  $15 \pm 0.2$  Ma with an initial propagation rate of  $\sim 300 \pm 50$  km/Myr. This one was referred to as the E-propagator in the work by *Hey et al.* [2010] but here we call it Loki, after the mischievous Norse god. Loki transfers lithosphere to North America and is a southward propagator so the offset between the propagating rift and the dying rift would have been a right-stepping transform (or non-transform) offset. Loki stalls between profiles 21 and 22 for  $\sim 0.9$  Ma (Figures 12b and 12c) where we detect a small transform-like discontinuity in the gravity data, herein termed *ponsu-transform* (ponsu is an Icelandic prefix meaning itty-bitty) (see the *ponsu-transform* in the gravity in Figure 11b), and then it continues on with a propagation rate of  $\sim 120 \pm 40$  km/Myr, transferring less lithosphere ( $\sim 4$  km versus  $\sim 5$ – $8$  km) to North America (Figure 12). The right-stepping *ponsu-transform* was formed as Loki stalled (Figure 12d). The bend in Loki's pseudofaults caused by the pause in propagation is shown schematically in Figure 12d and is evident in Figures 10a and 11a where it is shown as a schematic bend rather than a tiny offset. Interestingly, Loki's pseudofaults coincide with a major escarpment (the E-scarp in the works of *Vogt* [1971] and *Hey et al.* [2010]) on either side of the ridge.

[40] Two small propagators are initiated at the *ponsu-transform* after Loki has propagated through the survey area. At  $\sim 12.5 \pm 0.2$  Ma a northward propagator is initiated with a propagation rate of  $\sim 80 \pm 10$  km/Myr (Figures 10b and 11b). There is no evident pattern in the free air gravity (Figure 11b) coinciding with the pseudofaults of this propagator. At  $\sim 10.9 \pm 0.2$  Ma a southward propagator is

<sup>1</sup>Auxiliary materials are available in the HTML. doi:10.1029/2011GC003948.

**Figure 8.** (a–i) Profiles 17–25 modeled with the jump and magnetization parameters given in Table 6 and spreading rates from Table 4. Black is shipboard free air gravity, red is the magnetic anomaly data and blue is the model. Black and white boxes are normal and reversed magnetized blocks, respectively, following the bathymetry. Green solid and dashed vertical lines are pseudofaults and failed rifts, respectively. H = Hel, S = Sleipnir, F = Fenrir, and L = Loki propagators.

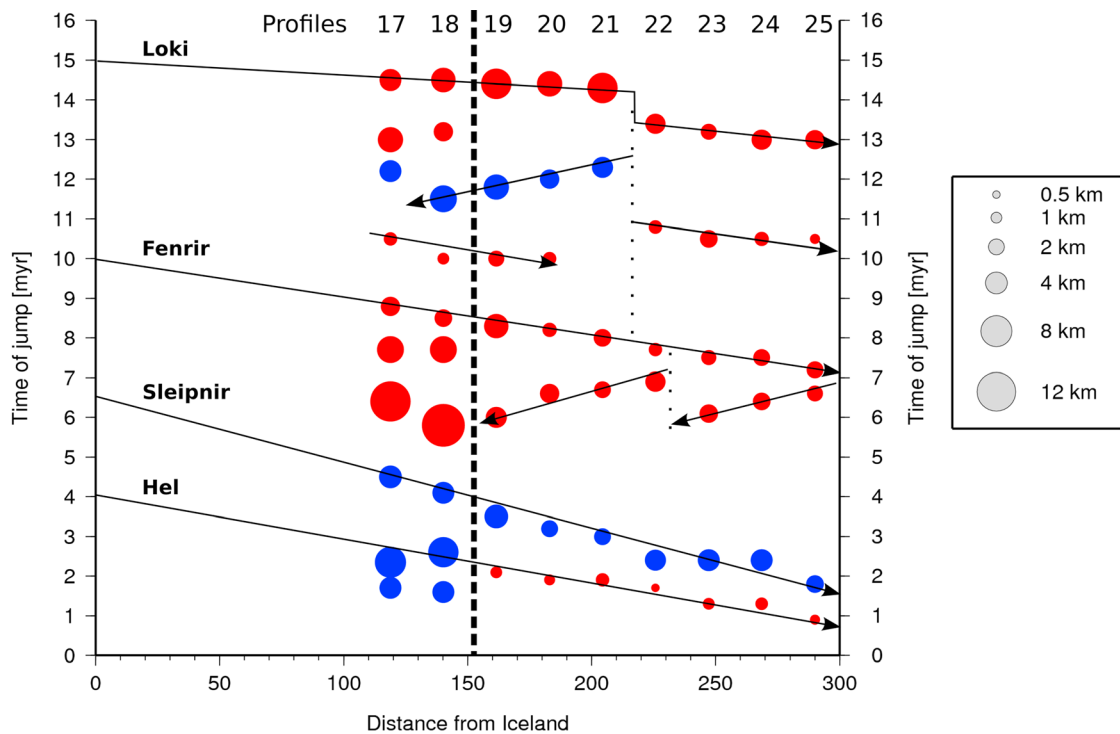


**Figure 9.** Time of jump from the magnetic models versus distance from the Reykjanes Peninsula (RP) (at 63.67°N/22.75°W) on Iceland. Red and blue circles correspond to jumps transferring lithosphere to North America or Eurasia, respectively. Arrows show direction of propagation. Solid lines are a linear interpolation of the southward propagating rifts extrapolated to the RP. Heavy dashed line separates the transitional profiles 17 and 18 from profiles 19 and south. Dotted lines are the locations of the two ponsu-transforms. Propagation rates are  $\sim 300 \pm 50$  km/Myr,  $\sim 120 \pm 40$  km/Myr,  $\sim 100 \pm 10$  km/Myr,  $\sim 60 \pm 10$  km/Myr and  $\sim 90 \pm 10$  km/Myr for Loki before the ponsu-transform, Loki after the ponsu-transform, Fenrir, Sleipnir and Hel, respectively.

initiated with the propagation rate of  $\sim 110 \pm 30$  km/Myr. The pseudofaults generated roughly follow the inward facing slope of a gravity ridge as seen in Figure 11b.

[41] An independent southward propagator is observed beginning on profile 17 at  $\sim 10.7 \pm 0.2$  Ma and stopping at profile 20 at  $\sim 9.8 \pm 0.2$  Ma, propagating at a rate of  $\sim 90 \pm 20$  km/Myr (Figure 10b). There is no evident pattern in the free air gravity (Figure 11b) coinciding with the pseudofaults of this propagator.

[42] The second continuous propagator, Fenrir (after the monstrous wolf in Norse mythology), left Iceland at  $10 \pm 0.2$  Ma with a propagation rate of  $\sim 100 \pm 10$  km/Myr if we assume it traveled in a linear fashion. Fenrir corresponds closely to the C propagator in the work of Hey *et al.* [2010] and transfers lithosphere from Eurasia to North America and re-organizes the ridge by eliminating the ponsu-transform (Figure 11c). The offset between the propagating rift and the dying rift would have been right-stepping. The pseudofaults generated by Fenrir coincide with a prominent and well established

gravity ridge on the North America plate and the inward facing scarp of a less well defined gravity ridge on the Eurasia plate.

[43] Two northward propagators are initiated after Fenrir, both transferring lithosphere to North America. A new ponsu-transform forms between profiles 22 and 23 at which one propagator is initiated at  $\sim 7.1 \pm 0.2$  Ma and the other one is stopped at  $\sim 5.8 \pm 0.2$  Ma (Figures 10d and 11d). The propagation rates of both are  $\sim 60 \pm 20$  km/Myr. The pseudofaults of these two propagators follow minor gravity ridges on the North America plate, forming two small V's pointing to Iceland (opposite to the general trend of the V-shaped ridges pointing away from Iceland) (Figures 10d and 11d), suggesting that the V-shaped ridges are complex features affected by small scale complexities such as propagators.

[44] The third continuous propagator left Iceland at  $6.5 \pm 0.2$  Ma with a propagation rate of  $\sim 60 \pm 10$  km/Myr assuming a linear propagation rate. This propagator was referred to as the A-propagator in the work of Hey *et al.* [2010] but here we call it

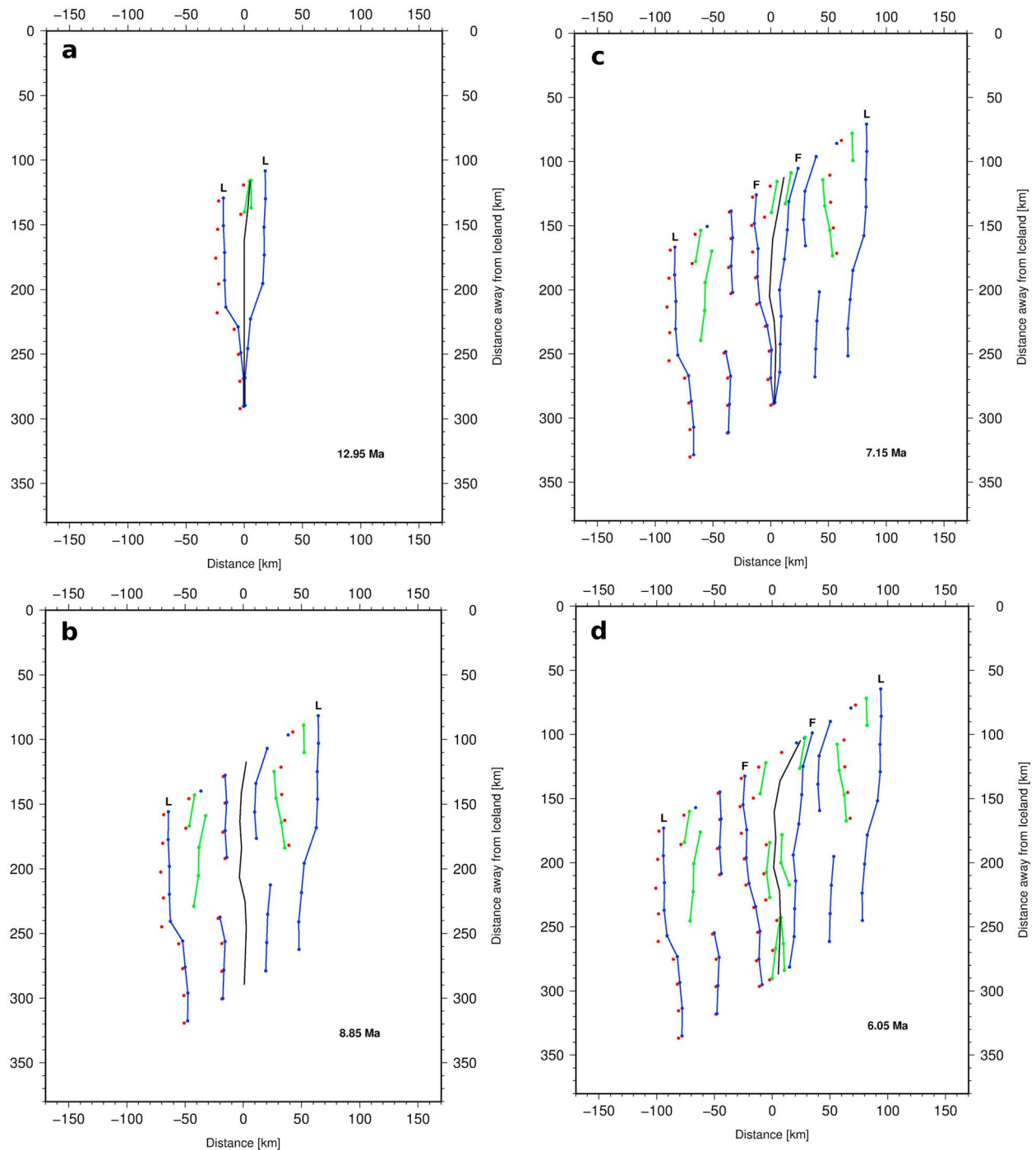


**Figure 10.** Cartoon showing the evolution of the Reykjanes Ridge. Horizontal axis is distance away from ridge and vertical axis is distance from the Reykjanes Peninsula. Green lines connect the pseudofaults of northward propagators, blue lines connect the pseudofaults of southward propagators, and red dots are failed rifts. Time of each snapshot is indicated by the number in the lower right corner. The ridge axis is shown by a black line and its geometry changes as new propagation events occur. L, Loki; F, Fenrir; S, Sleipnir; H, Hel. (a) After propagation of Loki. (b) Before Fenrir starts propagating. (c) After propagation of Fenrir. (d) Before Sleipnir starts propagating. The ridge axis at profile 17 is shifted to the right because of a big jump which later shows up in profile 18. (e) After propagation of Sleipnir, at the onset of Hel. (f) Present-day configuration.

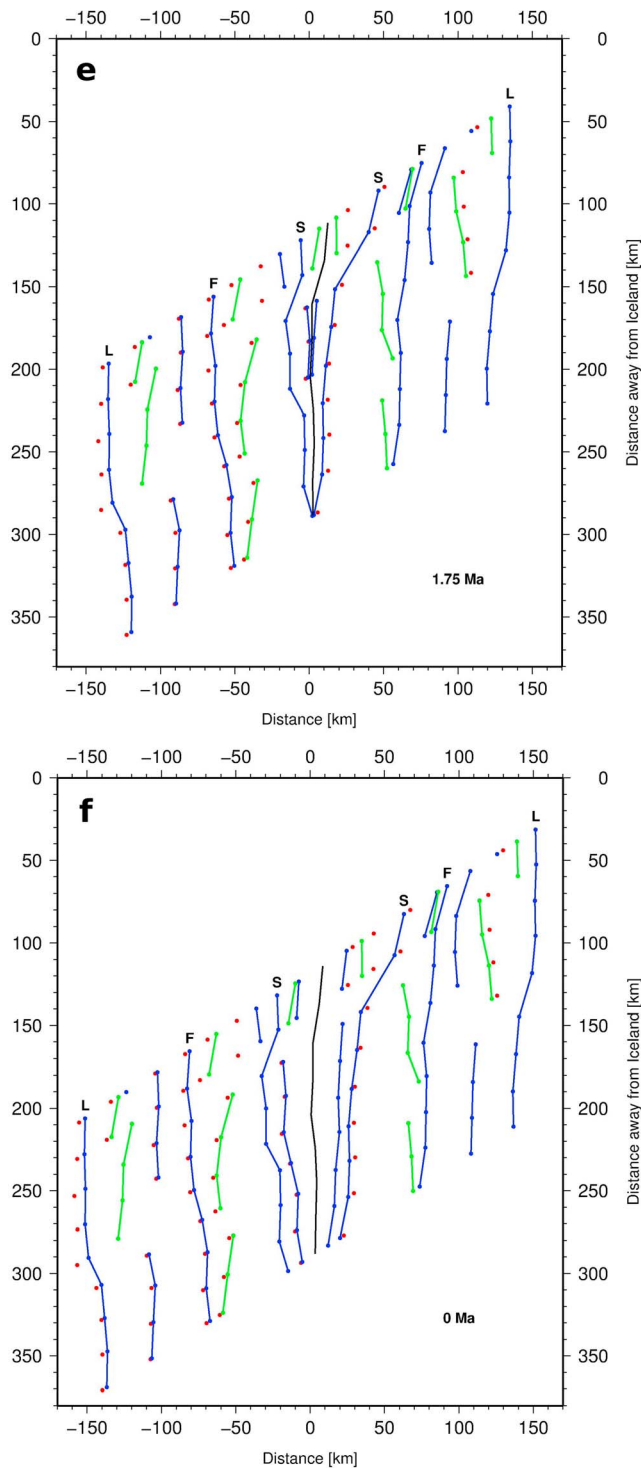


**Figure 10.** (continued)

Sleipnir after Odin's horse in Norse mythology. Sleipnir transfers lithosphere from North America to Eurasia, opposite to what *Hey et al.* [2010] found, and the offset between the propagating rift and

dying rift would have been a left-stepping one. The pseudofaults generated by Sleipnir coincide with the edges of the gravity ridge high (termed the A scarps in the works of *Vogt* [1971] and *Hey et al.* [2010]) in

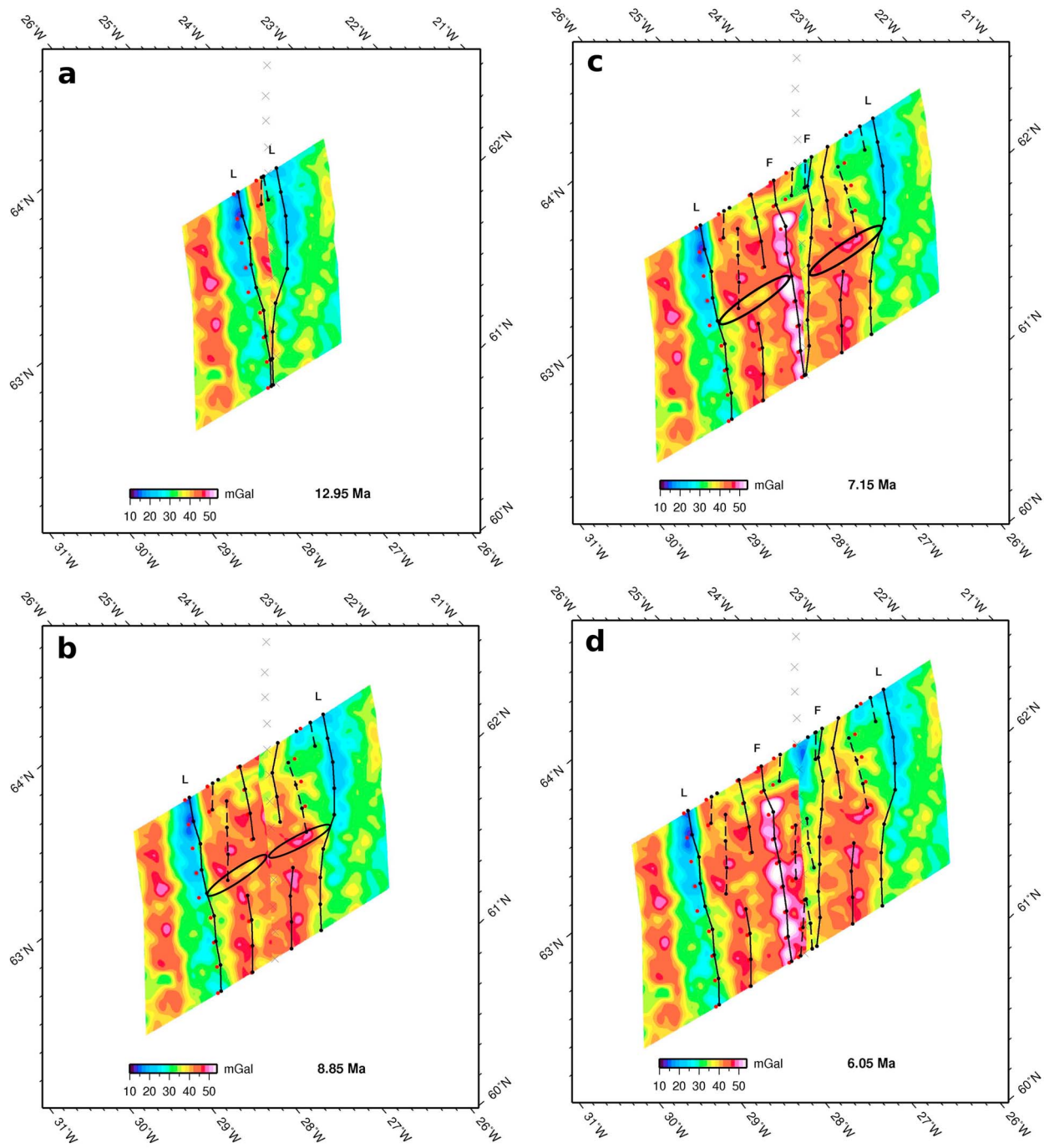


**Figure 11.** Snapshots of the evolution of the Reykjanes Ridge. Overlaid on satellite gravity [Sandwell and Smith, 2009] are pseudofaults (black circles) connected by solid and dashed lines for southward and northward propagators, respectively. Red circles are failed rifts. For each time the gravity is gridded in the area bounded by 19 Ma, the current time and profiles 17 and 25 on each ridge flank; the two areas are then rotated toward each other to close the space between the ridge and the areas. Time of each snapshot is indicated by the number in the lower right corner. L, Loki; F, Fenrir; S, Sleipnir. (a) After propagation of Loki. (b) Before Fenrir starts propagating. (c) After propagation of Fenrir. (d) Before Sleipnir starts propagating. The ridge axis at profile 17 is shifted to the right because of a big jump which later shows up in profile 18. (e) After propagation of Sleipnir, at the onset of Hel. (f) Present-day configuration.

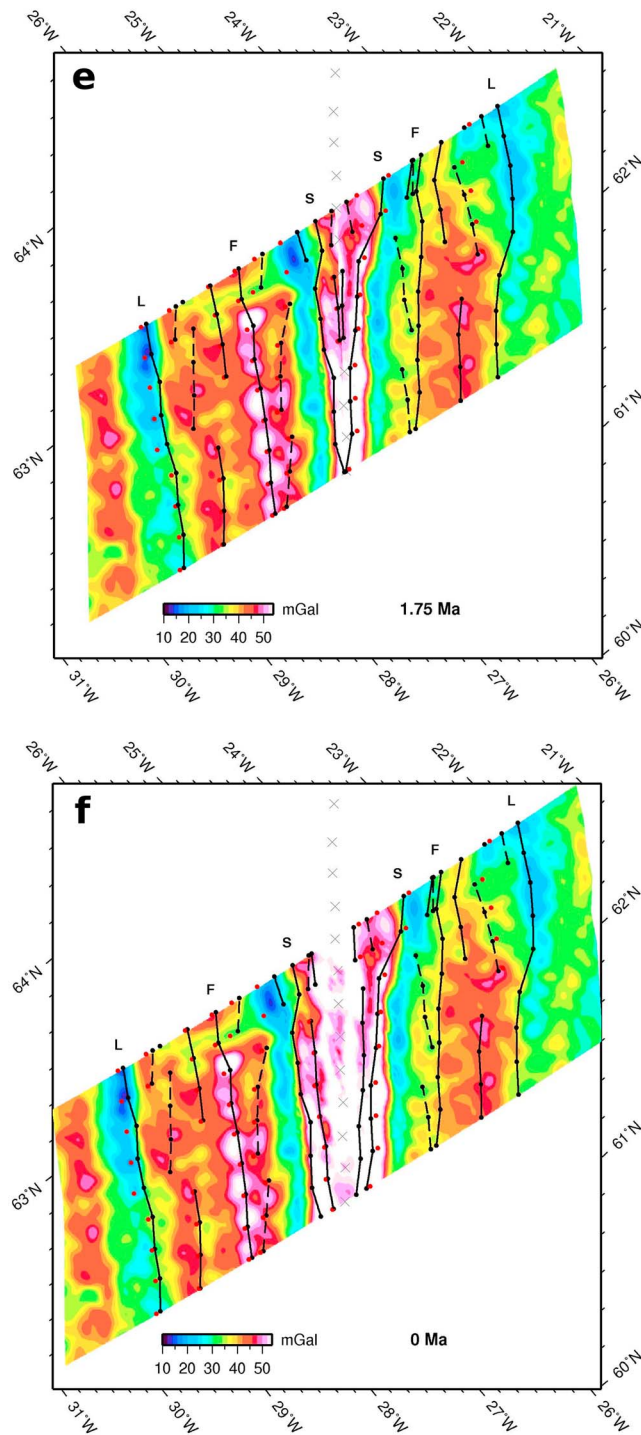


**Figure 11.** (continued)

the free air gravity (Figure 11e) on either side of the ridge. Similarly to Fenrir, Sleipnir eliminates the ponsu-transform and its pseudofaults coincide with a gravity ridge.

[45] The fourth continuous southward propagator left Iceland at  $4.0 \pm 0.2$  Ma with a propagation rate of  $\sim 90 \pm 10$  km/Myr, if assumed to propagate linearly. This propagator was referred to as the A'

**Table 8.** How Names of Major Propagators Relate Between Studies and a Hypothesized Related Ridge Jump on Iceland

This Study	Hey <i>et al.</i> [2010]	Ridge Jump on Iceland
Loki	E	Vestfirðir
Fenrir	B	?
Sleipnir	A	Snæfellsnes-Skagi
Hel	A'	?

propagator in the work of Hey *et al.* [2010] but here we call it Hel, after Loki's daughter in the Norse mythology. Hel transfers lithosphere from Eurasia to North America, opposite to what Hey *et al.* [2010] found, and the offset between the propagating rift and dying rift would have been a right-stepping offset.

[46] We agree with Hey *et al.* [2010] that the two youngest propagators produce jumps with opposite senses of asymmetry. The main difference between this study and that of Hey *et al.* [2010] is that we use the center of the Brunhes rather than the topography

to define the axis, and we do not assume that the A scarps are pseudofaults, although both studies assume the A scarps must be the same age, a major constraint on the magnetic anomaly modeling. Our interpretation of slightly different positions for the axis and the A scarps leads to a different pattern of young PRs than previously suggested, and provides a better fit to the anomaly data.

[47] Kleinrock *et al.* [1997] found propagation rates on the Mid-Atlantic Ridge (at ca. 26°–27°N) of 14–40 km/Myr and >75 km/Myr for two of their best identified propagators. Our rates are comparable to the faster one.

### 7.3. Transitional Profiles 17–18

[48] The jump pattern in this area is more complex than in the southern part of the survey area. There are a few key observations about this area that should be mentioned. First, the A-scarp curves out on the Eurasia plate north of profile 19 but not on the North America plate indicating that the crustal accretion in profiles 17 and 18 is different from the

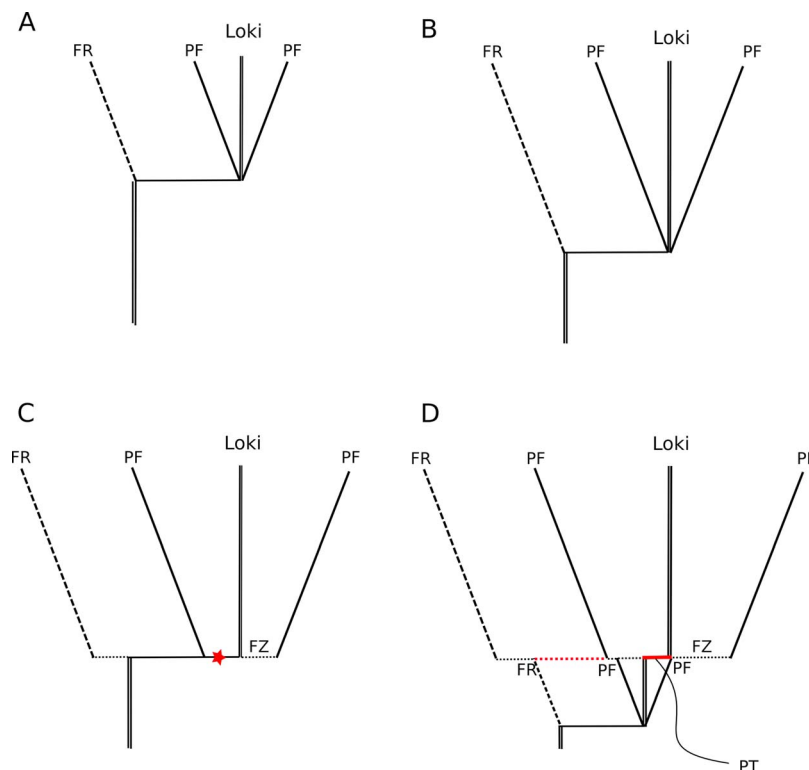


**Figure 12.** Schematic illustration of propagation of Loki. (a) Tectonic settings as Loki propagates from Iceland, transferring lithosphere to the North American plate. (b) Loki stalls. (c) As Loki is stalled the pseudofaults and failed rift spread away from the ridge. The red star indicates where Loki will continue propagating. (d) Loki continues to propagate but starts from the middle of the offset. A right-stepping ponsu-transform is created and there is a step in the pseudofaults at its location. The red dashed fracture zone (FZ) is a transform fault that got frozen into the North America plate as Loki continued propagating. FR, failed rift; PF, pseudofault; PT, ponsu-transform; FZ, fracture zone.

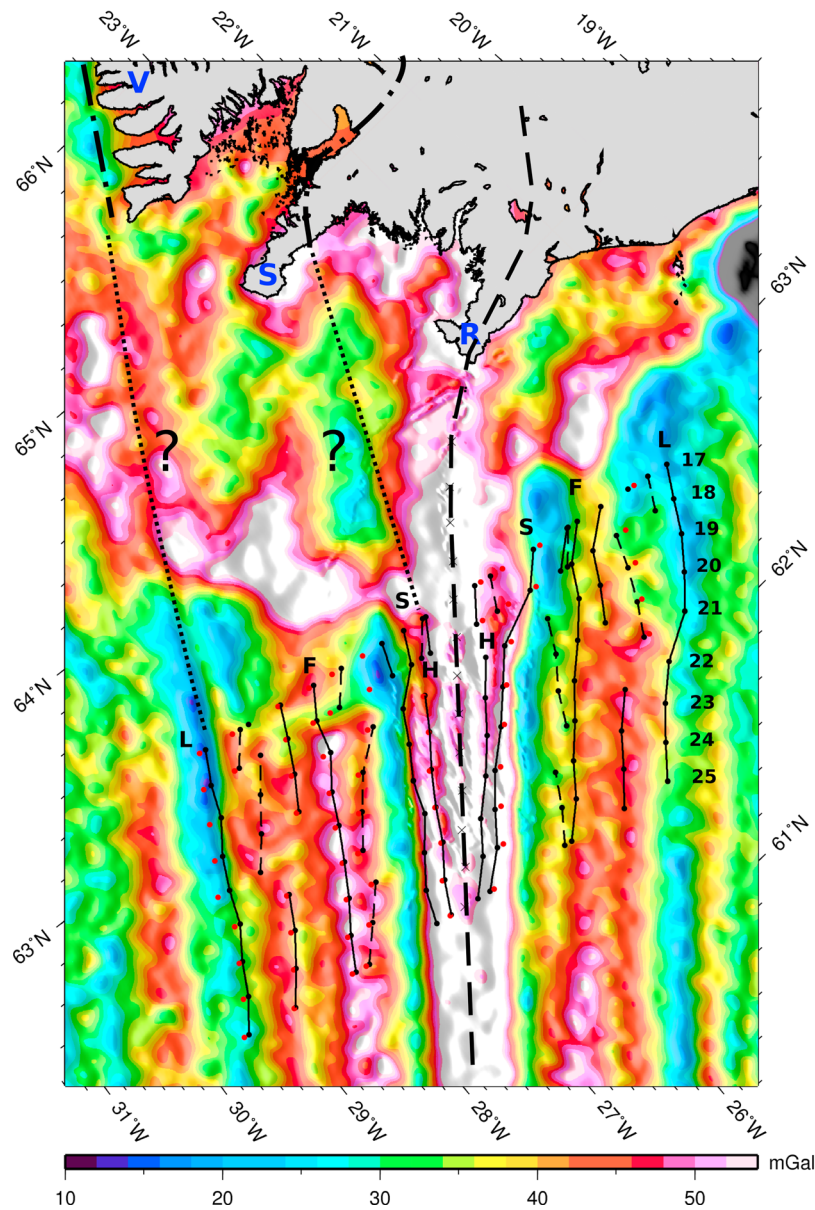


**Figure 13.** Satellite gravity and tectonic boundaries near Iceland [Sandwell and Smith, 2009]. Oblique Mercator projection. Pseudofaults and failed rifts predicted by our magnetic models are shown; solid lines connect the pseudofaults of southward propagating rifts, dashed lines connect pseudofaults of northward propagators, and red dots are failed rifts. Heavy dashed line is the Reykjanes Ridge and its extension up to Iceland; dash-dotted lines are the locations of the paleo-spreading centers in Iceland and dotted lines are an attempt to trail the paleo-spreading centers down to our survey area. Numbers indicate the location of our profiles (17–25). V, Vestfirðir; S, Snæfellsnes; R, Reykjanes Peninsula; L, Loki; F, Fenrir; S, Sleipnir; H, Hel.

area to the south where the A-scarp is much more linear. Secondly, a circular structure interpreted as a central volcano [Höskuldsson *et al.*, 2010] (centered on 63° 10' N and 25° 30' W), is apparent from the free air gravity at the ridge axis in profiles 17 and 18 (Figure 13) which differs considerably from the southern profiles where the free air gravity shows lineations subparallel to the ridge. A third

observation is that the pattern of the free air gravity on the ridge flanks changes drastically on profiles 17 and 18. A long gravity low along profile 18 on North America is present and the gravity ridges on the Eurasia side are not detectable. These observations suggest a different and a more complex crustal accretion process along profiles 17 and 18 compared to the profiles to the south.

[49] The most prominent differences on profiles 17 and 18 are the relatively large jumps (13–15 km) occurring at ~6 Ma transferring lithosphere from Eurasia to North America (Figure 9; two large red circles with no line drawn through them). They coincide with a gravity low on the North America plate (Figures 11f and 13) but interestingly jumps of this size are not observed farther south.

[50] Furthermore, there are several jumps we have not been able to attribute to a propagator. These jumps need to be there in order for the magnetic models to produce good fits to the anomaly data. As mentioned before, it is often plausible to take a jump and break it down to several smaller ones. Also, by reducing the size of one jump an adjacent jump can be made bigger (or smaller if it is transferring lithosphere in the opposite direction) and thus the amount of asymmetry is kept constant.

[51] The sense of asymmetry in this area is also distinctly different from the rest of the survey area. The youngest three jumps on these two profiles transfer a total of ~15 km of lithosphere to Eurasia within the first 4 Ma compared to 0.8–3.4 km for the southern profiles, explaining the curving of the A scarp on the Eurasia plate.

[52] We observe Loki, Fenrir and Sleipnir in our magnetic models for profiles 17 and 18 but we do not observe Hel, although as stated above we think that it propagated through profiles 17–25. The amount of lithosphere that is being transferred to North America by Hel is very little (~1 km) and the magnetic signal arising from the propagation might therefore be contaminated by complex crustal accretion processes (e.g., increased outward displacement) specifically because the A scarp on the Eurasian plate curves out right at profiles 17 and 18.

## 8. Discussion

[53] We provide generally excellent fits to our off-shelf magnetic profiles that are greatly improved over the ones in the work of *Hey et al.* [2010], particularly profiles 17 and 18, better establishing the rift propagation history on the Reykjanes Ridge. A striking new result is that propagating rifts can propagate north toward Iceland which would be counter intuitive for many because of the topographic gradient away from Iceland. A pulsing plume explanation for the origin of the VSRs [e.g., *Vogt*, 1971; *Vogt et al.*, 1980; *Smallwood and White*, 1998; *Jones et al.*, 2002] has been predominant for the past 40 years but *Hey et al.* [2010] suggested that the origin of the VSRs must at least

include rift propagation. *Hey et al.* [2010] discussed whether the plume pulses could drive the propagators. If plume pulses drive propagators they would all be southward propagating. As indicated by our magnetic models, northward propagators exist, and they would certainly not be driven by plume pulses, or an increased flow to the ridge after a ridge relocation on Iceland (as in the model of *Hardarson et al.* [1997]), indicating at least an additional controlling mechanism.

[54] The northward propagators tend to be shorter (crossing only a few profiles) and not as pronounced as the majority of the southward propagators (crossing all of our profiles). If Iceland plume pulses drive southward propagators then two sets of driving mechanisms for propagators exist: well established southward propagators (Loki, Fenrir, Sleipnir and Hel) driven by plume pulses re-organizing the Reykjanes Ridge eliminating ponsu-transforms, and shorter rift propagations driven by something else.

[55] The VSRs are not simple southward pointing Vs. Figure 13 shows the pseudofault and failed rift pattern predicted by our magnetic models in relation to Iceland superimposed on free air gravity [*Sandwell and Smith*, 2009]. Pseudofaults of southward and northward propagating rifts are connected with solid and dashed lines, respectively, and failed rifts are plotted as red dots. If the VSRs are plume pulses we would expect to see linear symmetrical gravity ridges subparallel to the Reykjanes Ridge but counter to that prediction the gravity ridges are not symmetric about the ridge axis. Their amplitude is greater on the North America plate where the majority of the failed rifts are located and there is a gap in the gravity ridges between profile 19 and the shelf edge which we explain by a fundamental difference in propagation history north and south of profile 18. *Jones and MacLennan* [2005] noted asymmetry of the Iceland shelf about the Reykjanes Ridge which can be seen in the free air gravity. The shelf reaches ~50 km further south on North America compared to Eurasia supporting the overall asymmetric accretion behavior of the Reykjanes Ridge. A pulsing plume would not cause asymmetric accretion but rift propagation would, so something would have to be added to the pulsing plume hypothesis to produce the observed asymmetry.

[56] The two ponsu-transforms we have identified independently with our magnetic models are observable in the free air gravity. The older ponsu-transform was active 8–14 Ma ago and was located

between profiles 21 and 22 (Figure 9). A discontinuity in the gravity ridges is seen in the reconstruction snapshot at 8.85 Ma (Figure 1b) as a linear feature paralleling the flowline of the Reykjanes Ridge. On the North America side it is a low and on the Eurasia side it is a high. Two propagators originate from this ponsu-transform and the Loki propagator stalled here for  $\sim 0.9$  Ma (Figure 12) causing the amount of lithosphere Loki transferred to the North American plate to decrease. As Fenrir propagated south the older ponsu-transform was eliminated. The younger, and smaller, ponsu-transform was active 5–7 Ma ago and was located between profiles 22 and 23. After Fenrir propagated down the survey area a well established gravity ridge subparallel to the Reykjanes Ridge formed on North America (Figure 11c). The younger ponsu-transform formed a little later (Figure 11d) from which one northward propagator was initiated at  $\sim 7.1$  Ma and at which a different one was eliminated at  $\sim 5.8$  Ma.

[57] Outward displacement has been reported to increase on the Mid-Atlantic Ridge from the Azores to the Reykjanes Ridge [DeMets and Wilson, 2008]. Outward displacement affects the location of pseudofaults determined from magnetic modeling and generally the greater the outward displacement the farther out the pseudofaults should be. The pseudofaults in our magnetic modeling therefore appear to be closer to the ridge by the value of the outward displacement. For the Reykjanes Ridge that value could be as high as  $\sim 5$ – $6$  km [DeMets and Wilson, 2008].

[58] The contamination coefficient is an indicator of smoothness of the magnetic data. Table 6 shows the contamination coefficient used for profiles 17–25. The smaller it is the more suppressed the high frequencies are in the data and therefore small reversals are less detectable. There is not a clear gradient or change along the ridge in the contamination coefficient, suggesting that small scale accretion complexities are present independent of distance from Iceland.

## 9. Unresolved Puzzles

[59] The results of the magnetic modeling suggest many more questions. These mostly come from observations we cannot explain by our present rift propagation model.

1. Bad fits at the end of profiles. As mentioned above we stop our magnetic modeling at  $\sim 15$  Ma

because of the limitation of our data coverage. A large scarp can be seen in the bathymetry of profiles 18–25 at  $\sim 210$ – $220$  km distance from the axis on the North America plate and if we had data coverage  $\sim 50$  km further out we would be able to model this area. Greater data coverage would further the understanding of the origin of the V-shaped ridges and the asymmetrical accretion of the Reykjanes Ridge.

2. The flowline-parallel gravity low on profile 18. Why would a gravity low persist for millions of years in one place on the plate boundary and only be noticeable on one ridge flank (the North American flank, see Figure 13)? This low is not an artifact in the satellite gravity data because it is observable in the shipboard gravity data as well (Figure 8b).

3. Large jumps not extending all the way through our survey area. The two  $\sim 15$  km jumps that transfer lithosphere to the North American plate at  $\sim 6$  Ma in profiles 17 and 18 are not traceable further south. The zone of transferred lithosphere located on the North America plate coincides with a very deep gravity low (Figure 13). Something must have caused the plate boundary to shift abruptly toward the east at  $\sim 6$  Ma when the big jumps occurred, and then slowly relocate back west, through three smaller jumps which transferred lithosphere back to the Eurasian plate (Figures 9 and 13). This same evolution is not observed to the south.

4. Propagation direction. Rift propagation has most commonly been observed to occur away from hot spots [Hey and Vogt, 1977; Delaney et al., 1981; Vogt et al., 1983; Schilling et al., 1985; Naar and Hey, 1991; Wilson and Hey, 1995], probably because of gravity spreading stresses caused by the topographic gradient away from hot spots [Phipps Morgan and Parmentier, 1985], but rift propagation has also been recorded to occur toward hot spots [Wilson and Hey, 1995; Barckhausen et al., 2008; Mihut and Müller, 1998] into a hotter, weaker lithosphere. It is therefore still poorly understood what controls the direction of propagation.

5. Fundamental difference between transitional and southern profiles. Both the free air gravity anomaly and jump pattern in the transitional profiles (17 and 18) differ highly from the southern profiles. A fundamental difference must exist in the crustal accretion processes between these two areas. The transitional profiles border the Iceland shelf which might be the cause of complex crustal accretion processes.

6. Asymmetric gravity amplitude about the Reykjanes Ridge. Sediments which derive from Iceland and blanket the Eurasia plate would tend to elevate the free air gravity signal and reduce the relative amplitudes between the troughs and the ridges. If the crustal thickness and bathymetry are the same on the ridge flanks we would expect to see higher free air gravity amplitudes on the Eurasia plate, which we do not for reasons still unknown. The most notable difference is in the gravity ridge that coincides with the pseudofaults of the Fenrir propagator (Figure 13).

## 10. Relation of Offshore and Onshore Rift Relocations

[60] The Eastern and Northern Volcanic Zones in Iceland have been propagating away from the Iceland hot spot [Sæmundsson, 1979; Schilling *et al.*, 1982; Hardarson *et al.*, 1997; Einarsson, 2008] and propagation to the southwest Iceland shelf has been hypothesised to match observed magnetic anomalies on the Iceland shelf [Kristjánsson and Jónsson, 1998]. Figure 13 shows the rift propagation on the Reykjanes Ridge suggested by this study in relation to Iceland. Dash-dotted lines on Iceland indicate locations of paleo-spreading centers [Sæmundsson, 1974]. We have suggested a relation (Table 8) between the paleo-spreading centers and our results with dotted lines extending from Iceland down to our survey area. The gravity scarp following the North America pseudofault of Loki can be traced on to the shelf to the paleo-spreading center of Vestfirðir as a gravity escarpment. As the Vestfirðir paleo-spreading center became extinct a propagator might have been initiated because a local change in the tectonic geometry limited the supply of magma down the ridge, as proposed by Hardarson *et al.* [1997]. Figure 9 shows that by linearly extrapolating the Loki propagator to Iceland it would have left at  $\sim 15$  Ma which coincides roughly with the extinction age of the Vestfirðir paleo-spreading center dated at  $\sim 15$  Ma [Sæmundsson, 1974]. Similarly, as the Snæfellsnes-Skagi paleo-spreading center became extinct a propagator might have been initiated with a pseudofault coinciding with the gravity step indicated by the dotted line from the Snæfellsnes peninsula. The North America pseudofault of Sleipnir could be linked to this event. Figure 9 shows that by linearly extrapolating the Sleipnir propagator to Iceland it would have left at  $\sim 6.5$  Ma which coincides roughly with the extinction age of the Snæfellsnes-Skagi paleo-spreading center dated at  $\sim 7$  Ma [Sæmundsson, 1974].

[61] If these speculations are correct then we can predict the existence of an unknown paleo-spreading center in Iceland between the Vestfirðir and Snæfellsnes-Skagi paleo-spreading centers which would have become extinct at  $\sim 10$  Ma when Fenrir left Iceland (Figure 9).

[62] Based on the gravity patterns associated with the northward propagators, which began after Fenrir propagated through the survey area, we predict that other northward propagators will be discovered south of our survey area where similar complicated gravity ridges, wider to the north than to the south, exist (Figure 13).

## 11. Conclusions

[63] We have attempted to accurately model the Reykjanes Ridge magnetic anomalies south of Iceland. These models strongly suggest rift propagation both toward and away from Iceland, explaining the observed asymmetric lithospheric accretion. Four major southward rift propagations extend through our entire survey area and all but the second most recent propagator transfer lithosphere to the North American plate. Several small scale rift propagations are observed, including northward propagations suggesting that the evolution of axial volcanic ridges complicates the rift propagation evolution. If plume pulses drive southward propagators, two different driving mechanisms for propagators must exist. There is a major difference in the crustal accretion asymmetry between the area immediately off the Iceland shelf and further south, both in the rift propagation pattern and the free air gravity lineations. Furthermore, we identify two small offset features coined *ponsu-transforms*, from which rift propagation is sometimes initiated and sometimes eliminated. The pattern of the VSRs is not symmetric or identical about the Reykjanes Ridge and the VSRs are not linear continuous features. Also, we have identified northward pointing Vs in the free air gravity and a major flowline-parallel free air gravity low, re-enforcing the conclusion that the VSRs are not simple features. Our rift propagation model provides excellent fits to magnetic data and provides a self-consistent model for the evolution of the Reykjanes Ridge during the past 15 Ma.

## Acknowledgments

[64] We thank the government of Iceland for permission to work in Iceland waters and the Iceland Coast Guard for emergency assistance. We thank the Captain and crew of the R/V

Knorr, A. Simoneau, R. Laird, A. Dorsk, P. Lemmond, E. Caporelli, D. Fornari, A. Shor, R. Herr, Th. Högnadóttir, M. Gudmundsson, E. Sturkell, for expedition help. We thank C. DeMets for providing new poles of rotation and expertise on the outward displacement phenomenon. We thank T. Björgvinsson for help with scripting and W. Roger Buck and Del Bohnenstiehl for reviews. All figures were made using The Generic Mapping Tools of P. Wessel and W. Smith. This work was supported by NSF grant OCE-0452132, a fellowship from Nordvulk, teaching assistanceship from the Department of Geology and Geophysics at the University of Hawai'i, and a grant from the Graduate Student Organisation at the University of Hawai'i.

## References

- Albers, M., and U. Christensen (2001), Channeling of plume flow beneath mid-ocean ridges, *Earth Planet. Sci. Lett.*, *187*(1–2), 207–220.
- Atwater, T., and J. Mudie (1973), Detailed near-bottom geophysical study of the Gorda Rise, *J. Geophys. Res.*, *78*(35), 8665–8686.
- Barckhausen, U., C. Ranero, S. Cande, M. Engels, and W. Weinrebe (2008), Birth of an intraoceanic spreading center, *Geology*, *36*(10), 767.
- Caress, D., H. Menard, and R. Hey (1988), Eocene reorganization of the Pacific-Farallon spreading center north of the Mendocino fracture zone, *J. Geophys. Res.*, *93*(B4), 2813–2838.
- Christie, D., B. West, D. Pyle, and B. Hanan (1998), Chaotic topography, mantle flow and mantle migration in the Australian–Antarctic discordance, *Nature*, *394*(6694), 637–644.
- Delaney, J., H. Johnson, and J. Karsten (1981), The Juan de Fuca–hotspot–propagating rift system: New tectonic, geochemical, and magnetic data, *J. Geophys. Res.*, *86*(B12), 11,747–11,750.
- DeMets, C., and D. Wilson (2008), Toward a minimum change model for recent plate motions: calibrating seafloor spreading rates for outward displacement, *Geophys. J. Int.*, *174*(3), 825–841.
- DeMets, C., R. Gordon, and D. Argus (2010), Geologically current plate motions, *Geophys. J. Int.*, *181*(1), 1–80.
- Einarsson, P. (2008), Plate boundaries, rifts and transforms in Iceland, *Jokull*, *58*, 35–58.
- Goodliffe, A., B. Taylor, F. Martinez, R. Hey, K. Maeda, and K. Ohno (1997), Synchronous reorientation of the woodlark basin spreading center, *Earth Planet. Sci. Lett.*, *146*(1–2), 233–242.
- Hardarson, B., J. Fitton, R. Ellam, and M. Pringle (1997), Rift relocation—A geochemical and geochronological investigation of a palaeo-rift in northwest Iceland, *Earth Planet. Sci. Lett.*, *153*(3–4), 181–196.
- Hardarson, B., J. Fitton, and A. Hjartarson (2008), Tertiary volcanism in Iceland, *Jokull*, *58*, 161–178.
- Hayes, D. (1976), Nature and implications of asymmetric seafloor spreading—“Different rates for different plates”, *Geol. Soc. Am. Bull.*, *87*(7), 994–1002.
- Herron, E., and M. Talwani (1972), Magnetic anomalies on the Reykjanes Ridge, *Nature*, *238*, 390–392.
- Hey, R., and P. Vogt (1977), Spreading center jumps and subaxial asthenosphere flow near the Galapagos hotspot, *Tectonophysics*, *37*(1–3), 41–52.
- Hey, R., and D. Wilson (1982), Propagating rift explanation for the tectonic evolution of the northeast Pacific—The pseudomovie, *Earth Planet. Sci. Lett.*, *58*(2), 167–188.
- Hey, R., F. Duennebieer, and W. Morgan (1980), Propagating rifts on mid-ocean ridges, *J. Geophys. Res.*, *85*(137), 3647–3658.
- Hey, R., H. Menard, T. Atwater, and D. Caress (1988), Changes in direction of seafloor spreading revisited, *J. Geophys. Res.*, *93*(B4), 2803–2811.
- Hey, R., F. Martinez, A. Höskuldsson, and A. Benediktsdóttir (2010), Propagating rift model for the V-shaped ridges south of Iceland, *Geochem. Geophys. Geosyst.*, *11*, Q03011, doi:10.1029/2009GC002865.
- Höskuldsson, A., R. Hey, F. Martinez, and Á. Benediktsdóttir (2010), Njörður Central volcano, first direct evidence of shallow magma chambers on the Reykjanes Ridge, paper presented at 29th Nordic Geological Winter Meeting, Statoil, Oslo, 11–13 Jan.
- Ito, G. (2001), Origin of V-shaped Reykjanes ridges from a pulsing and dehydrating mantle plume, *Nature*, *411*, 681–684.
- Johansen, B., P. Vogt, and O. Eldholm (1984), Reykjanes Ridge: Further analysis of crustal subsidence and time-transgressive basement topography, *Earth Planet. Sci. Lett.*, *68*(2), 249–258.
- Jones, S. (2003), Test of a ridge-plume interaction model using oceanic crustal structure around Iceland, *Earth Planet. Sci. Lett.*, *208*(3–4), 205–218.
- Jones, S., and J. MacLennan (2005), Crustal flow beneath Iceland, *J. Geophys. Res.*, *110*, B09410, doi:10.1029/2004JB003592.
- Jones, S., N. White, and J. MacLennan (2002), V-shaped ridges around Iceland: Implications for spatial and temporal patterns of mantle convection, *Geochem. Geophys. Geosyst.*, *3*(10), 1059, doi:10.1029/2002GC000361.
- Kleinrock, M., B. Tucholke, J. Lin, and M. Tivey (1997), Fast rift propagation at a slow-spreading ridge, *Geology*, *25*(7), 639.
- Kristjánsson, L., and G. Jónsson (1998), Aeromagnetic results and the presence of an extinct rift zone in western Iceland, *J. Geodyn.*, *25*(1–2), 99–108.
- Lourens, L., F. Hilgen, J. Laskar, N. Shackleton, and D. Wilson (2004), The Neogene Period, in *A Geologic Time Scale 2004*, edited by F. Gradstein, J. Ogg, and A. Smith, pp. 409–440, Cambridge Univ. Press, Cambridge, U. K.
- Macdonald, K. (1977), Near-bottom magnetic anomalies, asymmetric spreading, oblique spreading, and tectonics of the mid-atlantic ridge near lat 37 {degrees} n, *Geol. Soc. Am. Bull.*, *88*(4), 541–555.
- Menard, H., and T. Atwater (1968), Changes in the direction of seafloor spreading, *Nature*, *219*, 463–467.
- Merkouriev, S., and C. DeMets (2008), A high-resolution model for Eurasia–North America plate kinematics since 20 Ma, *Geophys. J. Int.*, *173*(3), 1064–1083.
- Mihut, D., and R. Müller (1998), Volcanic margin formation and Mesozoic rift propagators in the Cuvier Abyssal Plain off Western Australia, *J. Geophys. Res.*, *103*(B11), 27,135–27,149.
- Morgan, W. (1968), Rises, trenches, great faults, and crustal blocks, *J. Geophys. Res.*, *73*(6), 1959–1982.
- Morgan, W. (1971), Convection plumes in the lower mantle, *Nature*, *230*, 42–43.
- Naar, D., and R. Hey (1991), Tectonic evolution of the Easter microplate, *J. Geophys. Res.*, *96*(5), 7961–7993.

- Parson, L., et al. (1993), En echelon axial volcanic ridges at the Reykjanes Ridge: a life cycle of volcanism and tectonics, *Earth Planet. Sci. Lett.*, *117*(1–2), 73–87.
- Phipps Morgan, J., and E. Parmentier (1985), Causes and rate-limiting mechanisms of ridge propagation: A fracture mechanics model, *J. Geophys. Res.*, *90*(B10), 8603–8612.
- Phipps Morgan, J., and D. Sandwell (1994), Systematics of ridge propagation south of 30 S, *Earth Planet. Sci. Lett.*, *121*(1–2), 245–258.
- Poore, H., R. Samworth, N. White, S. Jones, and I. McCave (2006), Neogene overflow of northern component water at the Greenland-Scotland ridge, *Geochem. Geophys. Geosyst.*, *7*, Q06010, doi:10.1029/2005GC001085.
- Poore, H., N. White, and S. Jones (2009), A Neogene chronology of Iceland plume activity from V-shaped ridges, *Earth Planet. Sci. Lett.*, *283*(1–4), 1–13.
- Sæmundsson, K. (1974), Evolution of the axial rifting zone in northern Iceland and the Tjornes fracture zone, *Geol. Soc. Am. Bull.*, *85*(4), 495–504.
- Sæmundsson, K. (1979), Outline of the geology of Iceland, *Jokull*, *29*, 7–28.
- Sandwell, D., and W. Smith (2009), Global marine gravity from retracked Geosat and ERS-1 altimetry: Ridge segmentation versus spreading rate, *J. Geophys. Res.*, *114*, B01411, doi:10.1029/2008JB006008.
- Schilling, J., P. Meyer, and R. Kingsley (1982), Evolution of the Iceland hotspot, *Nature*, *296*, 313–320.
- Schilling, J., H. Sigurdsson, A. Davis, and R. Hey (1985), Easter microplate evolution, *Nature*, *317*(6035), 325–331.
- Searle, R., and A. Laughton (1981), Fine-scale sonar study of tectonics and volcanism on the Reykjanes Ridge, *Oceanol. Acta*, *4*, 5–13.
- Searle, R., J. Keeton, R. Owens, R. White, R. Mecklenburgh, B. Parsons, and S. Lee (1998), The Reykjanes Ridge: Structure and tectonics of a hot-spot-influenced, slow-spreading ridge, from multibeam bathymetry, gravity and magnetic investigations, *Earth Planet. Sci. Lett.*, *160*(3–4), 463–478.
- Shih, J., and P. Molnar (1975), Analysis and implications of the sequence of ridge jumps that eliminated the Surveyor transform fault, *J. Geophys. Res.*, *80*(35), 4815–4822.
- Smallwood, J., and R. White (1998), Crustal accretion at the Reykjanes Ridge, 61°–62°N, *J. Geophys. Res.*, *103*(B3), 5185–5201.
- Smallwood, J., and R. White (2002), Ridge-plume interaction in the North Atlantic and its influence on continental breakup and seafloor spreading, in *The North Atlantic Igneous Province: Stratigraphy, Tectonic, Volcanic and Magmatic Processes*, edited by B. Bell and D. Jolley, *Geol. Soc. Spec. Publ.* *197*, 15–37.
- Stein, S., H. Melosh, and J. Minster (1977), Ridge migration and asymmetric sea-floor spreading, *Earth Planet. Sci. Lett.*, *36*(1), 51–62.
- Talwani, M., C. Windisch, and M. Langseth (1971), Reykjanes Ridge crest: A detailed geophysical study, *J. Geophys. Res.*, *76*(2), 473–517.
- Tisseau, J., and P. Patriat (1981), Identification des anomalies magnétiques sur les dorsales à faible taux d’expansion, *Earth Planet. Sci. Lett.*, *52*, 381–396.
- Vine, F. (1966), Spreading of the ocean floor: New evidence, *Science*, *154*(3755), 1405–1415.
- Vogt, P. (1971), Asthenosphere motion recorded by the ocean floor south of Iceland, *Planet. Sci. Lett.*, *13*(1), 153–160.
- Vogt, P., and G. Johnson (1972), Seismic reflection survey of an oblique aseismic basement trend on the Reykjanes Ridge, *Earth Planet. Sci. Lett.*, *15*(3), 248–254.
- Vogt, P., G. Johnson, and L. Kristjansson (1980), Morphology and magnetic anomalies north of Iceland, *J. Geophys.*, *47*, 67–80.
- Vogt, P., N. Cherkis, and G. Morgan (1983), Project Investigator-I: Evolution of the Australia-Antarctic discordance deduced from a detailed aeromagnetic study, in *Antarctic Earth Science*, edited by R. Oliver, P. James, and J. Jago, pp. 608–613, Cambridge Univ. Press, Cambridge, U. K.
- Weissel, J., and D. Hayes (1971), Asymmetric seafloor spreading south of Australia, *Nature*, *231*, 518–522.
- White, N., and B. Lovell (1997), Measuring the pulse of a plume with the sedimentary record, *Nature*, *387*(6636), 888–891.
- White, R. (1997), Rift–plume interaction in the North Atlantic, *Philos. Trans. R. Soc. London, Ser. A*, *355*(1723), 319–339.
- White, R., J. Bown, and J. Smallwood (1995), The temperature of the Iceland plume and origin of outward-propagating V-shaped ridges, *J. Geol. Soc.*, *152*(6), 1039–1045.
- Wilson, D., and R. Hey (1995), History of rift propagation and magnetization intensity for the Cocos-Nazca spreading center, *J. Geophys. Res.*, *100*(B6), 10,041–10,056.
- Wilson, D., R. Hey, and C. Nishimura (1984), Propagation as a mechanism of reorientation of the Juan de Fuca Ridge, *J. Geophys. Res.*, *89*(B11), 9215–9225.
- Wilson, J. (1963), A possible origin of the Hawaiian Islands, *Can. J. Phys.*, *41*(6), 863–870.